AN ANALYSIS OF AQUATIC VEGETATION

IN THE SAN MARCOS RIVER

USING SUAS

by

Alexa Lopez, B.S.

A thesis submitted to the Graduate Council of
Texas State University in partial fulfillment
of the requirements for the degree of
Master of Science
with a Major in Geography
August 2021

Committee Members:

Jennifer Jensen, Chair

Thom Hardy

Kimberly Meitzen

FAIR USE AND AUTHOR'S PERMISSION STATEMENT

Fair Use

Duplication Permission

DEDICATION

I am dedicating this to myself and all other Latinas who can feel alienated by academia. You belong. You go girl.

ACKNOWLEDGEMENTS

I would like to thank Dr. Jennifer Jensen, who helped guide this research and was a wonderful mentor and companion through this journey, thank you for your time, and patience with me as a navigated through a world completely unfamiliar from my own. Dr. Kimberley Meitzen for her insight on the SMR and her time to help me understand the ecology in the river system, your kindness was invaluable to this work, and I appreciate your time to help me become a better scientist. Dr. Thom Hardy for his time and continued efforts to help me talk with the right people, your knowledge and commitment to presenting scientifically backed bodies of work were a lesson that I needed. I would like to thank Kevin Colgan who went out during the hot summers to help create the flight paths and fly the Phantom DJI, you did not have to do this at all and yet you did. Thank you for that. The members of the MCWE Habitat Conservation Crew who extended their time and knowledge to me, specifically Tom Heard and Collin Garoutte. My boyfriend Roger who helped me study, gave me advice, and supported me through my thesis, this was the hardest task I have ever taken on and without you I am not sure how smoothly the process would have gone. Finally, my parents, Alejandro and Sylvia and my sister Genevieve for their continued support, love, and pride to get me through this. I am doing this because you all have inspired me and instilled the confidence necessary to go where no Lopez has gone before. Thank you all so much for your support on a task I at times thought would be impossible to complete.

TABLE OF CONTENTS

Page

LIST OF TABLES

Table **Page**

LIST OF FIGURES

Figure **Page**

LIST OF ABBREVIATIONS

Abbreviation	Description
ACE	Adaptive Cosine Estimator
AM	Agisoft Metashape
ANN	Artificial Neural Networking
DEM	Digital Elevation Model
EAA	Edwards Aquifer Authority
EAHCP	Edwards Aquifer Habitat Conservation Plan
ESA	Endangered Species Act
ExG	Excessive Green Vegetation Index
GCP	Ground Control Points
GIS	Geographic Information Sciences
GPS	Global Positioning System
LiDAR	Light Detection and Ranging
MCWE	Meadows Center for water & the Environment
MDE	Multinomial Distribution Equation
NDVI	Normalized Difference Vegetation Index
NGDRI	Normalized Green-Red Difference Index
NIR	Near Infra-Red
OBIA	Object-based Image Analysis
RF	Random Forests

RMSE	Root Mean Square Error
SAM	Spectral Angle Mapping
SMR	San Marcos River
sUAS	Small Unmanned Aerial Surveillance
SVM	Support Vector Machine
TWR	Texas Wild Rice

ABSTRACT

Recreational usage is one of the largest impacts to the endemic Texas wild-rice (TWR) on the San Marcos river (SMR). During the summer of 2020, the restricted use of public access points to the river systems allowed a unique view of how aquatic vegetation responds with little intervention from river users. This thesis utilized small unmanned aerial surveillance (sUAS) to capture ultra-high resolution imagery of the SMR. The method used for classification featured an object-based image analysis using random forest, an AI algorithm to classify the data. The classified data had an accuracy assessment done which indicated an accuracy range 75.72% - 80.57% with a Kappa range of .59 - .70. The classified imagery was then used in a change detection from July to August, August to September and July to September to determine the change in vegetation composition during the summer months. During the study period, there was expansion of stands that were identified as exclusively TWR, and the expansion of mixed vegetation stands, indicating the growth of the aquatic vegetation system. This study provided a continuous coverage of aquatic vegetation from a planar view using sUAS during a unique period where normally the river would have experienced its highest usage.

I. INTRODUCTION

Background

The spring-fed San Marcos River (SMR) begins within the city of San Marcos, Texas where it flows from the Edwards Aquifer Balcones fault zone and is one of the main groundwater discharges of the Edwards Aquifer (Musgrove and Crow, 2011; Ewing, 2008). In the past several years, the City of San Marcos has experienced a 4.4% average population growth per year, which is above the national average rate of 1.5% (Colby and Ortman, 2015; U.S. Census Bureau, 2017). The number of residents and tourists using the river for recreation continues to grow, fueling concerns that the activity may lead to degradation of the aquatic habitats and impacts to endangered species such as Texas wild rice (Zizania texana) (TWR) (Bradsby, 1994; Breslin, 1998; Mora et al., 2013).

Tubing is a popular recreational activity in central Texas and some cities with river systems that experience high usage have undertaken efforts to reduce littering and other damage from recreational impacts. Neighboring cities like New Braunfels, Texas have increased restrictions on commonly littered items (i.e., can ban; City of New Braunfels, 2020) while simultaneously increasing parking fees to $20 during the summer when usage is at its peak. As a result of these restrictions and parking costs, the SMR has experienced an additional increase in river use (TXP, 2017). This increased usage has directly impacted ongoing efforts to minimize negative effects on aquatic vegetation such as TWR (EAHCP, 2019). While the summer season is normally the busiest time of the year for recreation on the SMR, because of the COVID-19 pandemic, the SMR's public access points were closed which severely limited the presence of river users for two extended periods during 2020. It is hypothesized TWR may have expanded in the absence of heavy recreational usage during the summer of 2020.

The unique conditions of the SMR allows for the proliferation of endemic aquatic species. One of the most regularly monitored aquatic plant species is TWR which is found within the upper five kilometers of the San Marcos River and has been federally listed as an endangered species since 1978 (Terrell et al. 1978). As such, monitoring of the SMR is conducted on an annual and frequent basis. One way monitoring has been done is through small, unmanned aerial systems (sUAS). In the past several years, scientists have used sUAS to monitor aquatic vegetation growth over time in shallow, non-turbid waters (Chapra, 2014). sUAS have been utilized within the SMR to model habitat suitability of TWR and invasive, non-native aquatic species as well as to document aquatic habitat restoration work as part of the Edwards Aquifer Habitat Conservation Plan (EAHCP) (EAHCP, 2019). This study will use sUAS data to map aquatic vegetation in the San Marcos River with a focus on TWR and perform change detection analyses to determine if vegetation distribution expanded or contracted in the absence of public access to the river between July and September 2020. The unique circumstances resulting in restricted public access to the river due to COVID-19 provides an opportunity to document the SMR's aquatic vegetation in the absence of previous volumes of summer recreational usage,

Problem Statement

During the summer recreational season aquatic vegetation could be negatively affected due to the high density of river users. Previous studies have identified the distribution and dispersal of aquatic vegetation in the San Marcos River (Owens et al. 2001, Tolman 2013). In 2009, Hardy et al. (2010) documented stand-based percent cover of aquatic vegetation by using kayaks to collect geographic information system (GIS) data with a Global Positioning System (GPS) at high positional accuracy. They used the field data to create one-meter polygon shapefiles of aquatic vegetation (Hardy et al., 2010). Since 2009, as part of the Edwards Aquifer Recovery Implementation Plan (EARIP) and later beginning in 2012, the MCWE habitat conservation crew, aquatic vegetation monitoring in the river has been conducted on an annual and bi-annual basis for select reaches. While vegetation is being mapped yearly this is not done as a continuous set of data. The data collected is primarily point and polygon data representing discrete sampling of the SMR. This research consists of a sequence of sUAS mapped vegetation and provides information on the relationship of the aquatic vegetation community at a centimeter resolution in the study area over a set period of time.

Objectives

The goal of this research is to map the aquatic vegetation from sUAS imagery acquired between July and September 2020. The sUAS data will be classified using an Object-Based Image Analysis (OBIA) method to create a series of vegetation maps that document TWR presence and distribution. The vegetation maps will be used to conduct a post-classification change detection. This will provide a snapshot of the state of vegetation during an otherwise peak recreation season. Specifically, the research objectives include:

1. Acquire sUAS imagery between July and September 2020.

2. Classify/quantify the composition of vegetation stands as three classes; Mono (TWR only), Mixed (stands of TWR and other aquatic vegetation), and Non-TWR (stands that do not include any TWR).

3. Provide comparisons of vegetation stand distribution between data collection dates to characterize vegetation expansion/contraction from July-September 2020.

Justification

The results from this study will contribute to the ongoing effort of mapping TWR distribution in the SMR. This research could provide the City of San Marcos and conservation entities with useful data that describes the state of TWR distribution considering limited recreational usage.

Currently, the EAHCP has goals in place that focus on maintaining the health and growth of native aquatic vegetation including the removal of non-native species. Texas State University has implemented a sustained and systematic effort since 2013 for non-native aquatic vegetation removal and planting of native species with an emphasis on TWR. These efforts include on-going monitoring and maintenance of restored areas. This study will provide a time series of mapped vegetation expansion/contraction over three months when normally the river would experience the highest concentration of visitors. During the summer of 2020, river usage was extremely limited due to lack of public access points. Finally, the study area for this research has been designated an area of biological interest to the EAHCP and this data can be useful in further monitoring studies.

II. LITERATURE REVIEW

Historic Instances of Mapping *Zizania Texana*

TWR (Zizania texana) has been documented since 1892 when G. C. Nealy collected the first instance of TWR and labeled the species incorrectly as Zizania aquatica (Terrell et al., 1978). In July 1921, the second instance of the aquatic species was collected under the assumption that the plant was Zizania aquatica after collecting samples from the San Marcos River (Terrell et al., 1978) Ultimately, it was not until 1932 when an amateur botanist in San Antonio, W.A. Silveus, became the first person to define TWR as a distinct species (Silveus, 1933; Terrell et al., 1978). Since its discovery, TWR is still the only Zizania species to be found in Texas (Terrell et al., 1978). Consistent documentation of TWR by government entities did not begin until the late 1960s into the early 1970s with the Texas Water Development Board collecting data on TWR in 1968, the U.S. Department of the Interior conducting their own study from 1967-1971, and lastly with the U.S. Fish and Wildlife Service investigating TWR to be considered as an endangered species in 1976. TWR was eventually listed as an endangered species in 1978.

In 1973, Young et al. (1973) found that approximately 80% of the native plants in the river had been replaced by exotic species since 1930. This decline was mainly due to anthropogenic causes such as harvesting species for commercial aquarium plant suppliers, the creation of dams, competition from introduced invasive species like Indian Hygrophila (Hygrophila polysperma), and habitat destruction from dredging, erosion, dams, and pollution (Young et al., 1973). The decline in native vegetation included TWR, with a noticed decline in abundance from the 1930s with Silveus' observations well into the 1990s from Power et al.'s (1996) research on TWR (Power et al., 1996).

Recent Mapping Efforts

The research conducted from the 1990s to the present reflect changes in mapping methodologies associated with increased efforts to restore the aquatic plant species into a more native habitat by planting native species and removing invasive aquatic plants. In the early 1990s, Powers (1992, 1996, 1997, 1998) and Poole (1992, 1993, 1995, 1996) spent several years documenting the habitat characteristics of TWR.

In 1994 and 1997, Bradsby (1994) and Breslin (1996) published studies that evaluated the recreational usage of the San Marcos River system. Their studies found that the highest usage occurred during the summer and that groups who knew about TWR were less likely to cause damage compared to river users with limited or no knowledge of TWR ecology. Additionally, research found that key recreational activities such as playing with dogs, kayaks, and tubing contributed to the destruction of aquatic vegetation (Bradsby, 1994; Breslin, 1996).

By 1999, Poole and Bowels (1999) published a comprehensive habitat characterization of TWR with the Texas Parks and Wildlife under a grant through the U.S. Fish and Wildlife Service. This included the location, preferred soils, composition of stands, and preferred water depth and velocity of TWR. In the same year, Hardy et al. (1999) published a multi-year study mapping the aquatic vegetation of the river system using GIS and developing a habitat suitability model of the endangered species within the San Marcos River. This research has been expanded upon and now includes research on water quality monitoring, stand composition, and in situ vegetation measurements, many of these activities are included as a part of the EAHCP.

In 2001, Owens et al. (2001) published the dispersal of aquatic vegetation that was mapped during 2000, which noted an increase in biomass in the river. Saunders et al. (2001) quantified depth, velocity, and substrate to define a habitat suitability model of the TWR. They found that TWR preferred shallower depths of < 1 m and the macrophyte thrives in a velocity of 0.125 to 0.457 m/s (Poole and Bowles, 1999; Saunders et al., 2001). The shallow depth preference of TWR and historically low turbidity of the river system makes this an optimal setting when attempting to employ sUAS imagery to map aquatic vegetation. Hardy et al. (2009) extended the work of Saunders et al. (2001) and utilized a more precise approach to measuring depth and velocity. Hardy et al. (2009) mapped the spatial distribution of TWR in more detail by using 1 m polygons which included composition of vegetation stands using GPS; this greatly improved the spatial resolution of the previous mapping.

Tolman (2013) characterized TWR habitat by incorporating riparian shade in the habitat classification model. Under the assumption that light affects the location and growth of TWR, they identified suitable habitat areas using GIS modeling based on integrating hydraulic modeling, Light Detection and Ranging (LiDAR), densitometer readings, and field observations of TWR spatial locations. Tolman (2013) found that the presence of TWR is highly dependent on its accessibility to sunlight and that shade should be a factor when considering the habitat characterizations of TWR.

Since 2012, the EAHCP has published yearly reports detailing restoration of the San Marcos River and TWR. This is a multi-organizational effort, with teams from different partnerships, such as the City of San Marcos and the Meadows Center for the Environment to map and monitor keystone species and both the expansion and removal of aquatic vegetation in rivers like the San Marcos and the Comal. The EAHCP has a section dedicated to the enhancement and restoration of TWR which included on-going yearly monitoring (EAHCP, 2019).

Background on the EAHCP

The Edwards Aquifer Authority (EAA) is a water district that was established in 1993 by the Texas legislature. The EAA poses as the regulatory agency overseeing groundwater in the Edwards Aquifer (Patoski, 2021). Although the EAA was initially created to ensure flows in the Comal and San Marcos springs as part of a plan to ensure Texans have access to clean water through 2050, the EAA has grown into a much more involved organization. For the first 20 years since its establishment, the EAA spent time documenting, collecting and synthesizing data regarding the state of the habitats overseen by the EAA and the quantity of groundwater availability. In 2013, the Edwards Aquifer Habitat Conservation Plan was permitted and approved for habitat conservation in the area. This plan protects the endangered species that live in the Edwards Aquifer spring systems according to federal law while also ensuring that there is a reliable source of water in the area (Gulley, 2017).

Currently, the EAHCP operates with three main measures in place: habitat protection measures, flow protection measures and supporting measures. The focus of this research has more to do with EAHCPs supporting protection and habitat protection measures so those will be discussed more in depth. Flow protection measures include working with both residential and commercial communities to prevent over pumping of groundwater and to ensure the minimum flow is maintained for each endangered species in the area (EAHCP, 2020). Habitat protection measures cover conservation and restoration of a given river system to a more native habitat. The city of San Marcos and Texas State University signatory partners to the EAHCP and take part in implementing the habitat conservation plan and monitoring the species in the SMR. Habitat conservation measures include Texas wild rice Enhancement and Restoration (EAHCP §§ 5.3.1/5.4.1) through the planting of TWR, Management of Recreation in Key Areas (EAHCP §§ 5.3.2/5.4.2) by monitoring and documenting areas of biological importance, and Control of Harmful Non-Native and Predator Species (EAHCP §§ 5.3.9/5.4.13) by removing invasive, non-native species and vegetation mats on the river (EAHCP, 2019). A full list of the habitat protection conservation measures can be found in Appendix 5 of the EAHCP. Supporting measures are maintained through applied research, ecological modeling, and biological monitoring. The work done in this thesis will contribute to applied research and biological monitoring of an area on the SMR that has been considered biologically diverse, featuring an endemic species (TWR) and thus an area of importance.

Aquatic vegetation monitoring is done by BIO-WEST, Inc. using a 10-foot sit-in kayak with a plexiglass window for visual observations, a Trimble GPS and an external Tempest antenna set on the bow of the kayak for high accuracy (10-60 cm) data (BIO-WEST, 2020) The SMR was mapped by vegetation patches, with discrete dimensions being determined by the dominant species being identified within a patch compared to the surrounding vegetation. After this the kayak then maneuvered around the perimeter of the patch to create a vegetation polygon. (BIO-WEST, 2020) Only patches one-meter in diameter and greater were registered as a polygon, however all TWR is recorded with individual TWR plants too small to be delineated as polygons being recorded as discrete points.

TWR Characteristics

Texas Wild rice or *Zizania texana* is a perennial, aquatic macrophyte endemic to the upper 8 km of the San Marcos River (Oxley, Pendergrass and Power, 2004). Historically, since its discovery there had been severe decline of the species found in the river due to invasive species and lack of habitat conservation. Since the 1990s there has been significant expansion of the plant, with some of the largest populations occurring after habitat management was implemented. Characteristics of the species are defined by pollination, seeding, preferences, and a description of the macrophyte.

TWR can produce both sexually and asexually. TWR pollinates through wind streams with male anthers that release pollen and are carried by the wind to the stigmas of female flowers (Oxley and Power, 2004). TWR pollen is viable for a short period of time with decreased viability by the 10-minute mark from its release. The optimal time of its release is during pre-dawn hours, between approximately 2am-4am, when temperatures are cooler and the humidity is higher relative to the daytime (Oxley and Power, 2004). Another way TWR reproduces is through asexual reproduction. This occurs along the long grassy strands of the plant tillers, which are roots that grow after the initial seed's germination. Tillers become large enough to break off from the nodes along the culm of the plant and sink to the bottom of the river (Oxley, Power, 2004). These are referred to as root clumps or root balls and form a large portion of the TWR population. Due to the nature of its reproductive patterns, it is best if TWR grows in groups with greater pollination release occurring within plants of 40 or more with less than one meter in gaps between plants (Oxley, Pendergrass and Power, 2004).

Historically, it was assumed that TWR was in decline due to its lack of successful reproduction but upon further analysis additional factors have been considered barriers to successful reproduction. Habitat modification of the area creates fragmented, widely spaced stands. Floating vegetation mats, debris and non-native fauna create competition as well (Oxley, Pendergrass and Power, 2004).

Seed production is another essential component to the population of TWR. Peak production of seeds occurs during March to June. March to June was identified as having the greatest seed production, but this does not necessarily guarantee every seed will be a successful producer (Power, 2004). Successful seeds are indicated by their ability to sink. Heavier or more dense seeds can reach the floor of the riverbed and sprouting while floating seeds will not have the necessary resources to successfully germinate. This phenomenon is also influenced by seasonal variation, with 79% and 77% of seeds during the months of April and May respectively sank. For context, during the remainder of the year, more than half of all seeds floated when dropped in water (Power, 2004). While TWR can flower during every month in a year, the peak reproductive period is April, May, and June (Oxley, Power, 2004). Because of this, March through June is the most important time of the year to protect TWR from disturbance which directly interferes with reproduction but also happens to be the period where river users start going in large numbers.

TWR preferences include a large range of velocity, being found anywhere from 0.05 m3/s -.75 m3/s (Power 2004). There is no unsuitable location regarding velocity preferences in the study area. The depth preferences of TWR can have a relatively large range as well. TWR can grow as low as sunlight will penetrate. As Tolman (2013) indicated, light attenuation is a key-factor in the presence and growth of TWR. TWR has an optimal preference of 0.46-0.69 m (Saunders, 2001), but can be found up to 4.5-6 m in depth. After 1-2 m in depth TWR will no longer flower but it can reproduce asexually, in addition to this the growth of TWR will not be as dense as it would be closer to the surface with a greater availability of light. There is no location in the study area where the depth is too deep for TWR to be able to grow. One of the few constraints in the study area is the substrate preferences of TWR. TWR prefers fine to coarse substrate and will struggle to root in areas where the bedrock is primarily made of clay. It has been documented that TWR substrate preferences are towards sand and fine to small gravel also referred to as coarse to coarse-sandy soils (Saunders et al., 2001). There are some pockets of clay bedrock areas in the study area, in those locations TWR has difficulty rooting and growing.

Remote Sensing for Aquatic Vegetation

The use of sUAS to study aquatic vegetation stems from the mapping of wetlands, with the development of different vegetation indices that facilitate mapping emergent vegetation in shallow waters (Chabot et al., 2018). A review of classification methods highlights a transition between applications used in mapping wetland and agricultural vegetation and how they can be optimized for use in shallow waters with low turbidity

(Ma et al., 2017). For classifying aquatic vegetation, methods have been developed that implement pixel-based approaches for instances like mapping invasive species on lake shorelines (Hill et al., 2017). A frequently used method when classifying coverage is the object-based image analysis (OBIA). OBIA involves clustering of spectrally similar pixels to optimize spatial and spectral detail (Chabot et al., 2016). Due to its growing popularity, a template for mapping river landscapes using sUAS-derived high-resolution imagery was created by Rusnak et al. (2017).

OBIA for Mapping Aquatic Vegetation

Alternative and emerging methods to map aquatic vegetation include the use of satellite imagery such as Landsat (Song et al., 2018), MODIS (Liu et al., 2015), and Sentinel-2 (Katja et al., 2019). Another remote sensing approach includes utilizing high resolution imagery through Aerial Photography (Marshall and Lee, 1994). However, the focus for this research will utilize use of sUAS for data collection. Over the last decade, there has been an increased use of sUAS to map aquatic vegetation. Segmentation is the first step in the OBIA classification method. Pande-Chetri et al. (2017) used a multi-resolution segmentation approach with high-resolution imagery from a sUAS to define classes from more generalized features to specific plant types based on the utilization of machine learning classifiers such as support vector machine (SVM) and artificial neural networking (ANN). Overall, their SVM classification method had the highest accuracy of 70.78%. Visser et al. (2016) also took a multi-resolution segmentation approach. However, they used expert knowledge to manually define habitat locations and focused on a smaller area with an emphasis on defining diverse genetic species in small locations on rivers. The results showed a 61% accuracy using the OBIA method and supervised classification.

The utilization of vegetation indices may improve classification accuracy. Chabot et al. (2018) incorporated the use of an infrared sensor on the sUAS flight, which helped improve accuracy to 80-90% depending on the vegetation class. Jing et al. (2017) used a total of seven indices as part of a comparative study to determine which index is best at identifying differences in submerged aquatic vegetation. These included the Normalized Green-Red Difference Index (NGDRI), an index that is modeled after the Normalized Difference Vegetation Index (NDVI) which can separate aquatic plants from water and soils. The Excess Green Vegetation Index (ExG) doubles the values of the green band to highlight the difference between the red and blue bands in order to help further define vegetation that is present underwater. The results showed an overall accuracy of ~89% and a Kappa coefficient of 0.86 which is a statistical method that measures agreement between two rasters. In this case, the Kappa coefficient determines agreement of the classification of an image to ground truth data taken as a reference to how accurately the image was classified. Landis and Koch (1977) outlined the interpretation of a Kappa coefficient as: 0.01-0.20 slight; 0.21-0.40 fair; 0.41-0.60 moderate; 0.61-0.80 substantial; 0.81-1.00 almost perfect (Landis and Koch, 1977).

Husson, Ecke and Reese (2016) compared two classification algorithms, Random Forests (RF) and threshold classification in eCognition to map emergent vegetation at five sites. They found that more complex vegetation compositions resulted in lower accuracy. They also compared manual versus automated mapping and found that the manual mapping was more accurate due to user input. Flynn and Chapra (2014) compared classification systems for defining algal river coverage in shallow non-turbid rivers. They used the Adaptive Cosine Estimator (ACE) and Spectral Angle Mapper (SAM) algorithms. ACE was used by the researchers with the hypothesis that it would help differentiate green spectral responses associated with algae and SAM makes direct comparisons of predefined spectra with known classes. The results showed an accuracy of 90% for ACE and 92% for SAM.

III. METHODOLOGY

Study Area

The San Marcos River is a spring-fed system that has low turbidity, a mean flow rate of 4 m^3/s, and a mean temperature of 22˚C. These conditions provide suitable habitat for TWR. The study area includes the lower boundary of Sewell Park and extends downstream through City Park within the City of San Marcos to the first pedestrian walking bridge (Figure 1). The study area experiences high density recreational use and includes the Lions Club tube rental facilities on the left bank of the river and Dog Beach on the right bank with focused river access from both banks.

Figure 1. Study area within the San Marcos River. Launch point of the DJI Phantom 3 is denoted by a green star.

Data Collection

Field Data Collection

On July 3, 2020 ground control points (GCP) were collected which are locations in the study area that can be easily identified on the imagery and located accurately on a map (Jensen, 2004). When working with GCPs, two distinct sets of coordinates can be derived: image coordinates and map coordinates. The paired coordinates from multiple GCPs are used to derive geometric transformations to geometrically rectify the data into a given datum and map projection (Jensen, 2004). Image rectification may not remove all the distortion present from the orthomosaic but can significantly reduce the distortion and improves the positional accuracy of the data. Information on the positional accuracy for each orthomosaic image is provided in Table 2. Twenty-eight GCPs were collected in the field using a Trimble GeoXH GPS receiver. Each position was assigned a name, given a brief description, and was drawn with a notebook in the field. The points were uploaded into Microsoft Excel and a .CSV file was created and imported into Agisoft Metashape for image processing.

Image Data Collection

sUAS imagery was processed on three dates during summer 2020; July 13, August 24, and September 25, using a Phantom 3 DJI RGB sUAS were used in this study. Imagery was collected between the hours of 3:30-4:30 pm to prevent sun glare and to account for similar spectral responses. Each mission consisted of two flights; the first flight collected imagery from Dog Beach going upriver towards Sewell Park and the second flight launched from Dog Beach and extended downriver to the first pedestrian bridge within City Park (Figure 1).

During the month of September 2020, the city parks were re-opened for public access and the study area became difficult to capture due to increased river users (Table 1). Although multiple weeks of imagery were available from July and August, changes in expansion and contraction of aquatic vegetation occurs during longer time scales, as observed by Hardy et al. (2009). Due to this, and because each flight did not produce optimal imagery mainly due to dynamic weather causing spectral differences when creating orthomosaics, I determined one flight would be processed from each month. The flights selected for processing optimized image quality as determined by uniform illumination conditions for classification of the aquatic vegetation.

Table 1**.** Timeline of river access for the City of San Marcos from March-September 2020 and chosen flight classification date.

Date	Action
March 23, 2020	Public river access is closed for the first time due to COVID-19
May 22, 2020	Access to public river points is restored, people are allowed on the river through public access points.
June 25, 2020	Public river access on the San Marcos River is closed again due to an increase in COVID-19 cases.
July, 2020	Flights began July 3rd. Selected flight for classification: July 13th, 2020.
August, 2020	Selected flight for classification: August 24th, 2020.
September 16, 2020	Public river access is reinstated due to declining cases in the area.
September 25, 2020	Final flight for this thesis and flight selected for classification: September 25th, 2020

Reference Data

Reference data were obtained from BIO-WEST, an environmental planning and consulting firm that is partnered with the EAA to monitor the aquatic vegetation in the

SMR. Reference data were used during the accuracy assessment point creation to act as a guideline when determining accurately defined points. As an example if an object was classified as mixed, but the reference data determined that the object was a mono stand, the accuracy assessment point would then be classified as mono and the classified imagery would be considered incorrectly classified. Data attributes included the percentage of TWR coverage for each polygon and the associated aquatic vegetation found within the stands. The data were collected using a GPS receiver and stored as point and polygon shapefiles. Two data sets included 68 data points found in the study area collected August 6, 8, and 9 in 2019 and 159 polygon shapefiles with an average size of 35.92 m2 and a standard deviation of 192.85 m2 collected during August 3, 4, 5 in 2019. An additional 121 polygons were collected during August 3, 4, 5 in 2020 with an average size of 63.67 m2 and a standard deviation of 283.15 m2. Since 2019 data may not accurately represent vegetation in the river during this study period due to recreational usage, I only used vegetation polygons for reference if the polygon corresponded with vegetation visible in the sUAS imagery. The August 2019 data had greater change and the removal of polygons since over a year had passed after the data were collected. The August 2020 data were collected during the study period, this created an accurate representation to use when classifying the data and checking for accuracy and served as a great point of reference.

Additional reference data were created from in-person interviews with Dr. Meitzen over video conference on March 4, 2021, and at the study area on March 16th, 2021, and members of the MCWE habitat conservation crew at the study area on April 22, 2021, over email on May 4, 2021. In addition to the BIO-WEST data and on-site visits, reference data were also created by email communications discussing the nature of the orthomosaics though clarifying whether an area might have been defined as mixed or mono with the vegetation that can be identified through a planar view taken by the sUAS.

Data Analysis and Techniques

Image Processing

After each flight was completed, I transferred the data to a workstation to perform the orthorectification process. Orthorectification was completed in Agisoft Metashape (AM) using a batch process that aligned the photos, optimized the alignment, and built a dense point cloud. The imagery was georeferenced to the GCPs collected in the field on July 3, 2020. The points taken from the GCP collection were uploaded as XYZ data from a .CSV file and added onto the images opened in AM by their identifiable features.

For each data collection date, a dense cloud was created and examined to identify erroneous points (e.g., point well above or below the surface) and those points were manually removed. From the dense point cloud, a Digital Elevation Model (DEM) was created which is necessary to produce the orthomosaic. Using the DEM and the georectified images, an orthomosaic of each dataset was created. The final orthomosaics are ultra-high resolution rasterized images from each flight. Spatial resolutions of the final orthomosaics varied from 1.88 cm/pix – 2.03 cm/pix (Table 2). Each image was also provided with a root mean square error (RMSE) which indicates the error of positional accuracy plus or minus the RMSE.

Table 2. Orthomosaics used and their corresponding image resolution and RMSE.

Date	Resolution	RMSE
July 13, 2020	2.03 cm/pix	11.48 cm
August 24, 2020	1.93 cm/pix	12.62 cm
September 25, 2020	1.88 cm/pix	76.08 cm

Image Classification

The orthomosaic was exported into ArcGIS Pro as a raster and the raster was clipped to water's edge to exclude sidewalks, grass, manmade structures, and tree canopy. All data were projected to the NAD 1983 UTM Zone 14N coordinate system.

OBIA requires image segmentation prior to applying a classification algorithm. The Segmentation tool in ArcGIS Pro was used for segmentation. The segmentation tool has three main inputs: spectral detail, spatial detail, and minimum segmentation size. The spectral input defines the relative importance of separating objects based on color characteristics. Smaller values result in broad classes and more smoothing. Higher values are appropriate when discriminating between features having similar spectral characteristics; valid values range from 1.0-20.0 with step changes of 0.5 (ESRI, 2021). Since this research involves determining the differences between semi-submerged aquatic macrophytes which can appear spectrally similar, the spectral detail was set to a high value.

The spatial detail parameter focuses on the relative importance of separating objects based on spatial characteristics. Smaller values result in broad classes and more smoothing while higher values are appropriate for discriminating between features that are spatially small and clustered together (ESRI, 2021). Since the sUAS data had an ultra-high spatial resolution and the classes for comparison were stands of aquatic vegetation, the spatial detail parameter was also set to a high value. Valid spatial values range from 1.0-20.0, with step changes of 1.0. Minimum segment size considers mapping unit size and will filter out blocks of pixels that are smaller than the determined size. TWR has an average stand size of approximately 2.13 m long by 1m wide (Oxley, Powers 2004; Owens et al. 2001), and the resolution of the sUAS data is approximately 2 cm per pixel. Since this research is differentiating between stands of aquatic vegetation, with a specific focus on TWR, 2.13 m x 1 m at a resolution of 2 cm per pixel creates a rectangular shape that is approximately 3,500-4,000 pixels in size. This was the range used to determine the minimum segment size (Table 3) and helped with eliminating noise and aggregating spectrally similar areas on the river system. Since emergent root culms were too small to be detected, a smaller minimum segment size created noise and difficulty defining class features.

Table 3. Segmentation parameters for each classified image

Month	Minimum Segmentation Size	Spectral Detail	Spatial Detail
July	3,500	20.0	19.0
August	3,500	18.50	17.0
September	3,500	19.50	17.0

After an image was segmented, training samples were created. Training samples are a series of segments that correspond to the defined classes in the classification schema. The schema for classification was defined as: Substrate – 10, Non-TWR – 20, Mixed – 30 and Mono – 40. A description of each class is provided in Table 4. To ensure that spectral variability within the classes was accounted for, subclasses were identified (e.g., bright, and dark Non-TWR vegetation). Prior to final map production, the subclasses were merged to their general class.

Table 4. Class categories and class values

Class	Definition	Subclass Definition	Class Code
Substrate	Areas where there is no aquatic vegetation present	N/A	10
Non-TWR	Stands of mixed vegetation or stands of vegetation that contain no TWR	Non TWR Bright (21), Non-TWR Dark (22)	20
Mixed	Stands with TWR and other Aquatic vegetation	Mixed Bright (31) and Mixed Dark (32)	30
Mono	Stands of only TWR	TWR Bright (41) and TWR Dark (42)	40

After the classification samples were created, the image was classified using the Image Classification tool in ArcGIS Pro, with the Random Trees classifier (also known as Random Forests (RF)) method was chosen. RF is a statistical method that uses decision trees to determine the likelihood of an object belonging to a certain class (Breiman, 2001). This method classifies an image based on a random selection of training pixels where the number of pixels used is specified by the user. The process begins with creating a specified number of decision trees, which is the basis for a RF model. Decision trees define a pixel's classification by creating several rules ranked to determine the likelihood of a pixel belonging to a class. Rules create the "branches" of the decision tree. An example of a decision tree can be found in Figure 2. Each pixel being evaluated goes through several decision trees, with a class being returned based on the rules for a given tree; a collection of trees is what creates the "forest" in RF.

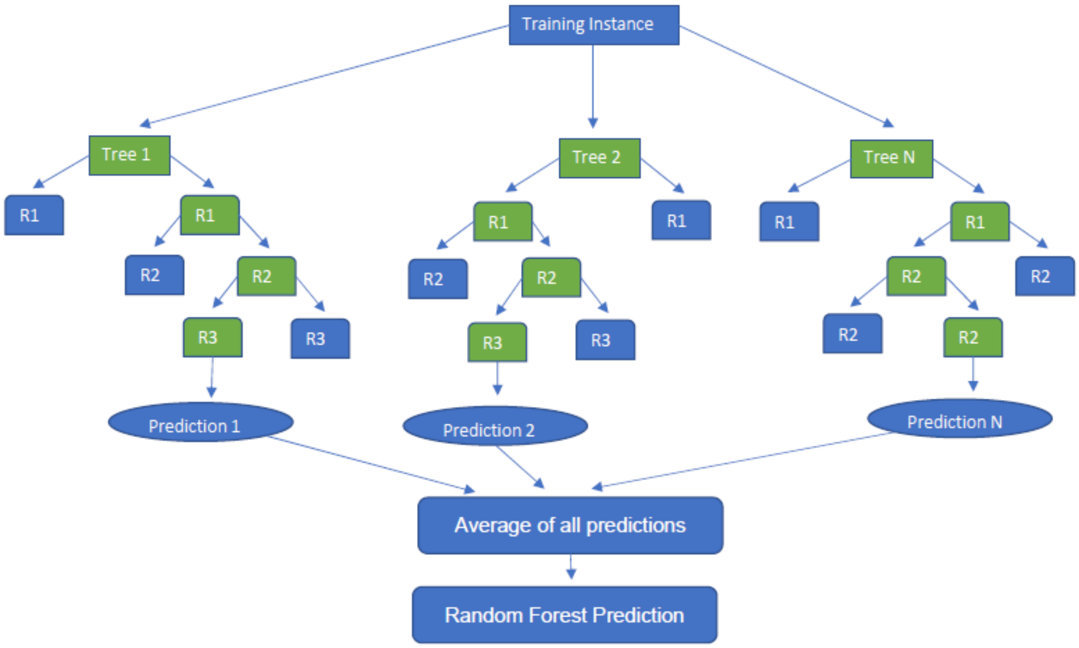

Figure 2. Random Forest conceptual model.

The RF algorithm in ArcGIS Pro requires five input parameters: Training Samples, Maximum Number of Trees, Maximum Tree Depth, Maximum Number of Samples per Class, and Segmented Image (optional). The training samples input is a polygon shapefile of the training samples. The maximum number of trees indicates the number of trees in a forest; the more trees used, the greater the potential accuracy (ESRI, 2021). Maximum tree depth defines the number of rules within each tree. The maximum number of samples is used for defining each class. For each image I chose zero to use all training samples to train the classifier. Finally, the segmented raster created from the orthomosaic was used for classification of each image date. Detailed information for each classified image is provided in Table 5. The raster derived from the classification tool provides two sets of information in the attribute table: class name, which describes the name of the class category, and class value, which is a long integer attribute that specifies the count of pixels within the classified image for each category.

Table 5. Image classification RF parameters

Orthomosaic	Max # of Trees	Max Tree Depth	Max # of Samples per Class
July 13, 2020	135	100	0
August 24, 2020	120	90	0
September 25, 2020	120	90	0

Map Validation

For the accuracy assessment, I targeted an 80% accuracy for the Mono class and 70-80% overall accuracy. Since the focus of this research is TWR, the Mono class was considered the most important and I wanted high agreement in the accuracy of that class being defined. The desired 80% accuracy was chosen based on the considerations of working with sUAS in a dynamic environment and based on existing literature. Ma et al. (2017) published a review of 220 papers that utilized OBIA using different sensors with the inclusion of sUAS and different supervised classification methods with considerations to RF. In the studies, RF had the highest mean classification accuracy of 85.81% (Ma et al., 2017). I aimed for an accuracy lower than this because many of the studies did not work in an aquatic environment which creates its own challenges for accurately classifying imagery.

Overall, the focus will be on the Kappa statistic to determine the agreement of the accuracy. A Kappa of 0.01 - 0.20 is slight agreement; 0.21 - 0.40 is fair agreement; 0.41 - 0.60 is moderate agreement; 0.61 - 0.80 is substantial agreement; 0.81 - 1.00 is almost perfect agreement (Landis and Koch, 1977). I aimed for a Kappa of 0.61 or higher to demonstrate substantial agreement of the classified images accuracy. I used the multinomial distribution equation (MDE) (Equation 1; Jensen 2004) to determine the number of samples necessary for a statistically objective accuracy assessment.

Multinomial distribution equation:

$$N=\frac{B\Pi_i(1-\Pi_i)}{b_i^2} \qquad \text{(Equation 1)}$$

Where:

$$B = \left({}^{\alpha}/_{k}\right) * 100$$

Where N represents the number of observations or samples, B represents the Chi-square critical value for alpha (α) divided by k multiplied by 100. Where α represents one minus the confidence desired for the map, in this research it was 1 - 0.80, and k is the number of classes which is four in this study. This is then multiplied by 100 and that number is used in a chi-squared right-tail distribution table with one degree of freedom. Π_i represents the class whose proportion of the map is closest to 50% and b_i represents the desired precision. In this study I chose a desired precision of five percent.

The Zonal Histogram tool obtains a count of the raster values from the classified data set. Each class is divided by the total count of pixels to identify the class proportions for the MDE (Equation 1). After this the MDE (Equation 1) was calculated. Since the size of each image varies due to tree canopy coverage, and the proportion of classes varied as well, the amount of sample points needed was different for each map output. A stratified random sampling design method was used to proportionally among the four classes. Samples required for each classified map accuracy assessment are provided in Table 6.

Table 6.: Minimum number of sample points required for a statistically substantial accuracy assessment using the MDE (Equation 1).

Image Date	Number of samples required
July	384
August	376
September	380

After identifying the amount of sample points needed for accuracy assessment, sample points were created using the Create Accuracy Assessment Points tool in ArcGIS Pro. Using the reference data provided by BIO-WEST, the interviews conducted in situ which involved going to specific portions of the study area to discuss the vegetation composition, the emails sent discussing the orthomosaic images and what the classification of a given area would be, and my visual interpretation of the imagery, each accuracy assessment point was assigned a reference value. After all reference values were assigned, I used the Compute Confusion Matrix tool to generate an accuracy assessment report.

The confusion matrix facilitates calculation of producer accuracy, user accuracy, overall accuracy, and an overall Kappa coefficient of agreement value. Producer accuracy indicates how effective the map classification was, and omission errors describe the percentage of pixels omitted from the correct class. User accuracy is a measure of how useful the data is to the user and commission error provides information on pixels included in a class they do not belong to. Overall accuracy describes the proportion of correctly classified objects. Kappa analysis measures the agreement of the classified map compared to the reference data and whether the agreement is based on chance. Kappa coefficients of agreement range from 0-1. The closer to 1 the Kappa statistic is, the stronger the agreement between the classified map and reference data. Upon achieving a satisfactory output, the workflow continued to the post-classification change detection of the classified imagery.

Change Detection

A post-classification change detection was conducted between three time periods: July 2020 to August 2020, August 2020 to September 2020, and July 2020 to September 2020. To be accurately compared, the images needed to be clipped and resampled to a similar resolution. The images were clipped to the September 2020 image since it had the smallest extent, and the images were re-sampled to the July 2020 image resolution since it had the largest pixel size of 2.03 cm/pixel. The September and August 2020 rasters were resampled with the Resample tool using the nearest neighbor resampling technique in ArcGIS Pro. Nearest neighbor does not change the value of the cells and minimizes the changes to pixel values. The July and August 2020 rasters were then clipped to the smallest extent using the Clip Raster tool.

The post-classification change detection was completed using ArcGIS Pro's Change Detection Wizard tool with categorical change. The process uses two rasters representing to and from data (e.g., from July to August). Next, the configure step identifies classes that will be used in the change analysis. In this case all four classes were used as indicators of change, so when filtering the data, the changed only option was used which showed which pixel values changed classes. Under the configure window there is one more output: Transition Class Color Method which specifies which method will be used to symbolize the pixels that have changed classes. Since this research looked at change from month to month, the 'to color' option was used. For example, if a pixel was classified as Mixed in July but Mono in August, the output was coded as Mono. The final step was the post processing window which can provide smoothing, but that option was not used in this research to leave the pixels unaltered. The data were exported as a raster and feature class and the change detection was complete.

IV. RESULTS

Image Classification

All three classified images had less than three percent of the image classified as Non-TWR, with July (Table 7), August (Table 8), and September (Table 9) totaling 2.24%, 1.6%, and 1.5%, respectively. For all three dates, TWR was the largest class with a value of 50.73% for July 57.23% for August and 55.39% for September. Substrate showed the greatest variation of change, with a 51.35% difference from the July classification (18.5%) to the September classification (9.5%). Classified maps for each image date are provided in Figures 3-5.

Table 7. Summary class counts and percentages for July 13, 2020.

Class	Count of pixels	Percentage of class coverage
Substrate	3,862,553	18.5%
Non-TWR	467,774	2.24%
Mixed	5,958,576	28.53%
Mono	10,596,163	50.73%

Table 8. Summary class counts and percentages for August 24, 2020.

Class	Count of pixels	Percentage of class coverage
Substrate	3,629,754	13.44%
Non-TWR	431,014	1.6%
Mixed	7,484,973	28%
Mono	15,454,093	57.23%

Table 9. Summary class counts and percentages for September 25, 2020.

Class	Count of pixels	Percentage of class coverage
Substrate	2,707,464	9.5%
Non-TWR	418,047	1.5%
Mixed	9,464,725	33.53%
Mono	15,633,669	55.39%

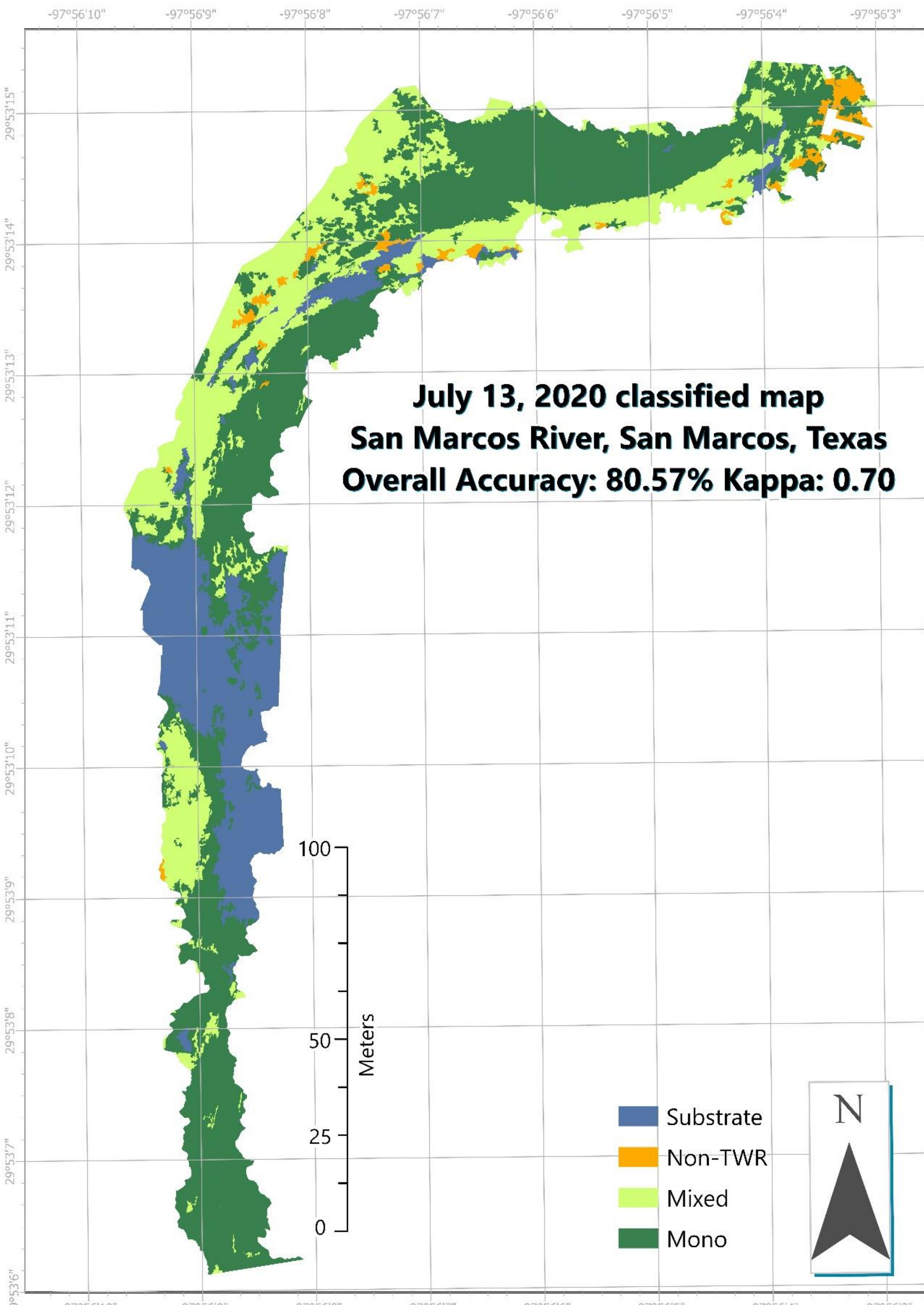

Figure 3. Classified map for July 13, 2020.

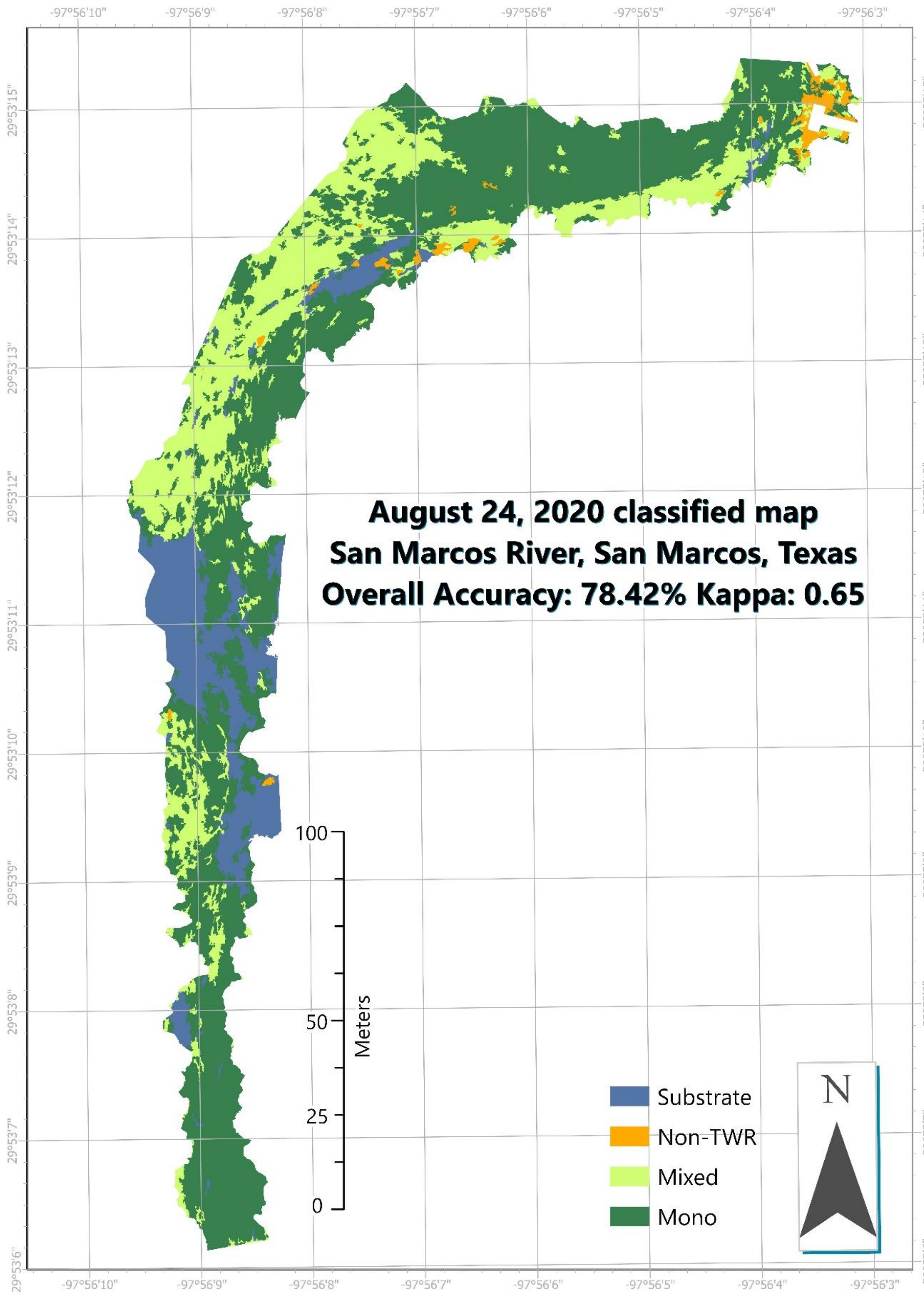

Figure 4. Classified map for August 24, 2020.

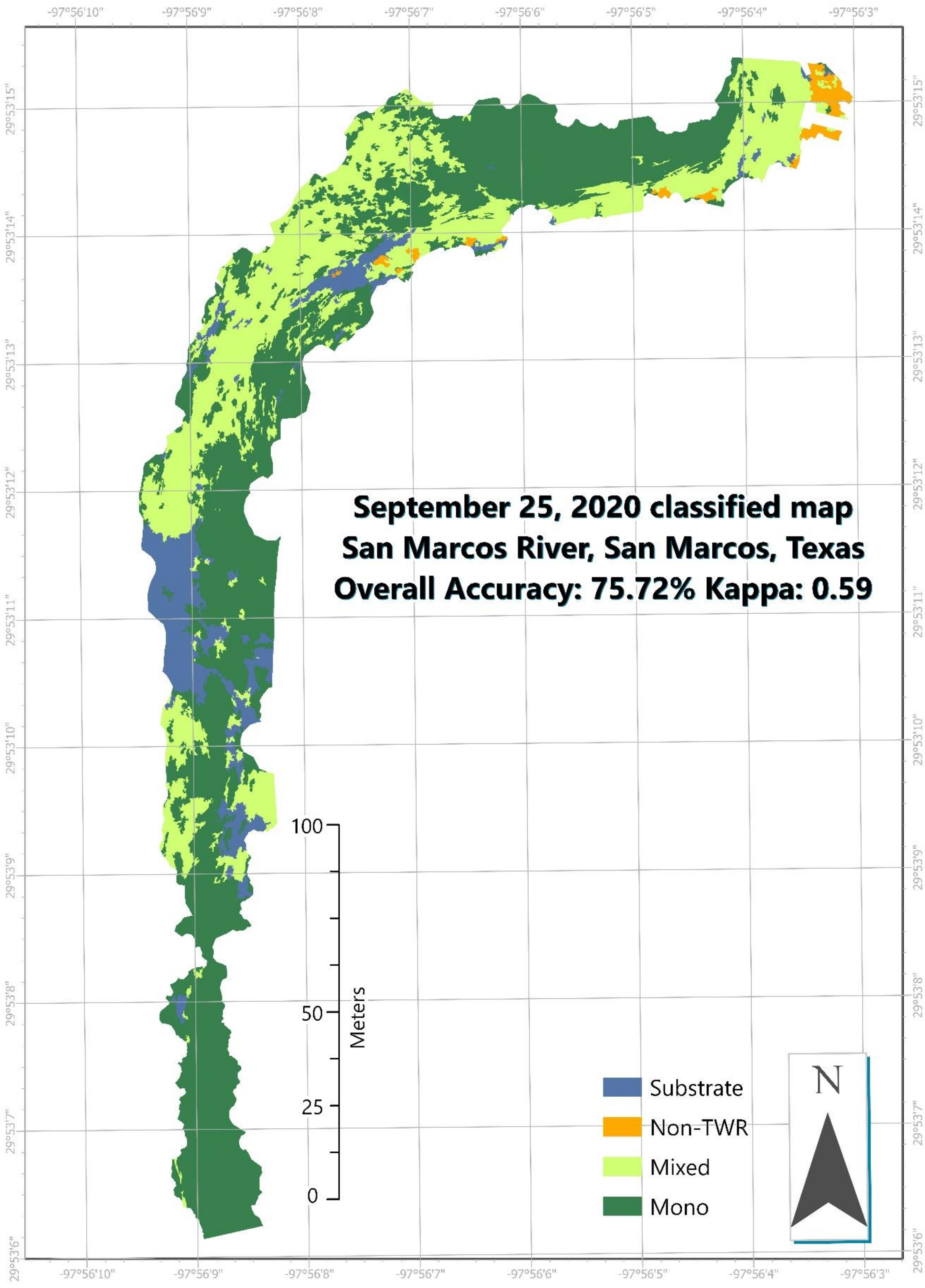

Figure 5. Classified map for September 25, 2020.

July and August had Kappa values of 0.70 and 0.65, respectively while September had a Kappa value of 0.59. Summary accuracy statistics are provided in Tables 7 – 9 for July, August, and September, respectively. The table is a confusion matrix which indicates the sample points and what they were classified as during the accuracy assessment points, as an example, in Table 10 the first row indicates that the substrate class was given 71 points in total, and 66 out of 71 points were classified accurately, indicating a user accuracy of 92.96%. The mono class is highlighted as this is the class had the highest desired accuracy and was the main focus of this research. July and September both had user and producer accuracies for Mono over the desired 80% at 81.54% and 85.95% for July, and 84.76% and 83.57% for September, while August had a producer accuracy of 87.56% and a user accuracy of 78.60%. Overall accuracy of the classified images ranged from 75.72% in September to 80.57% in July.

Table 10. Classified raster accuracy assessment for July 13, 2020.

Class	Substrate	Non-TWR	Mixed	Mono	Total	User Accuracy	Kappa
Substrate	66	1	0	4	71	92.96%	
Non-TWR	0	5	4	1	10	50.00%	
Mixed	1	7	81	21	110	73.64%	
Mono	5	4	27	159	195	**81.54%**	
Total	72	17	112	185	386		
Producer Accuracy	91.67%	29.41%	72.32%	**85.95%**		**80.57%**	
Kappa							**0.70**

Table 11. Classified raster accuracy assessment for August 24, 2020.

Class	Substrate	Non-TWR	Mixed	Mono	Total	User Accuracy	Kappa
Substrate	47	1	1	2	51	92.16%	
Non-TWR	1	8	0	1	10	80.00%	
Mixed	2	7	74	21	104	71.15%	
Mono	10	4	32	169	215	**78.60%**	
Total	60	20	107	193	380		
Producer Accuracy	78.33%	40.00%	69.16%	**87.56%**		**78.42%**	
Kappa							**0.65**

Table 12. Classified raster accuracy assessment September 25, 2020.

Class	Substrate	Non-TWR	Mixed	Mono	Total	User Accuracy	Kappa
Substrate	29	1	6	0	36	80.56%	
Non-TWR	0	10	0	0	10	100.00%	
Mixed	11	8	73	35	127	57.48%	
Mono	8	0	24	178	210	**84.76%**	
Total	48	19	103	213	383		
Producer Accuracy	60.42%	52.63%	70.87%	**83.57%**		**75.72%**	
Kappa							**0.59**

Change Detection

For the July to August 2020 map comparison (Table 10), pixels that were identified as Mono in July and Mixed in August accounted for the greatest change, at 11.04%. In the change detection, 73.86% of pixels from July to August remained unchanged. For the August to September 2020 change detection (Table 11) the largest change occurred between pixels that were identified as Mixed in August and became Mono in September (11.75% of pixels) and was the single greatest class variation in any of the images. Overall, from August to September, 67.79% of pixels did not change. The greatest changes occurred between July and September 2020 (Table 15). Where 66.93% of the pixels found within the July to September imagery went unchanged. Maps of the change detection from month to month are provided in Figure 5.

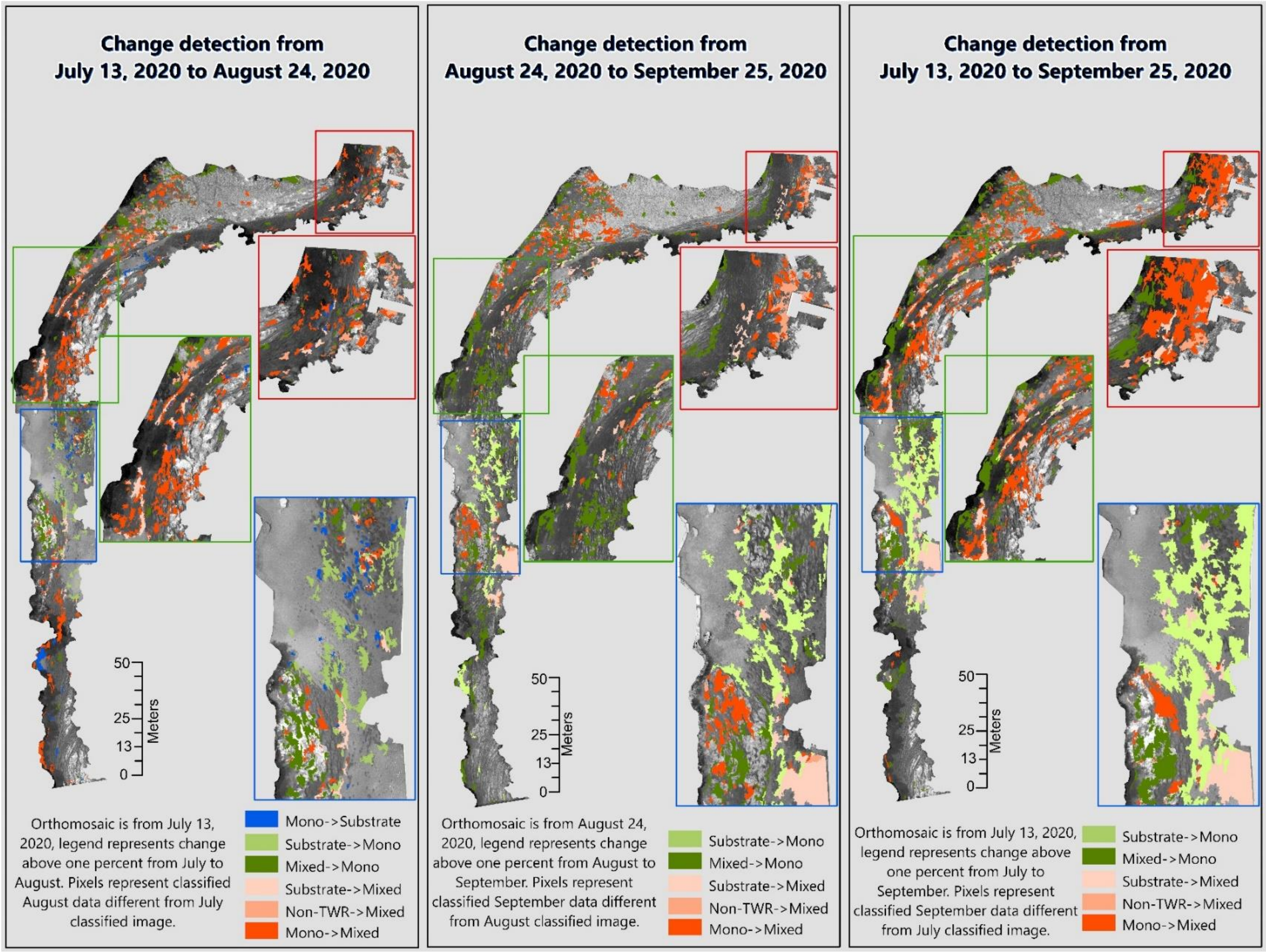

Figure 6. Change detection map with changes greater than one percent

Table 13. Change detection from July 2020 to August 2020. Top three largest changes are in bold. Class mapping codes are included with the class name.

Class Change	July Class	August Class	Percent
Substrate->Non-TWR	Substrate 10	Non-TWR 20	0.20%
Substrate->Mixed	Substrate 10	Mixed 30	1.77%
Substrate->Mono	**Substrate 10**	**Mono 40**	**2.86%**
Non-TWR->Substrate	Non-TWR 20	Substrate 10	0.01%
Non-TWR->Mixed	Non-TWR 20	Mixed 30	1.34%
Non-TWR->Mono	Non-TWR 20	Mono 40	0.37%
Mixed->Substrate	Mixed 30	Substrate 10	0.65%
Mixed->Non-TWR	Mixed 30	Non-TWR 20	0.39%
Mixed->Mono	**Mixed 30**	**Mono 40**	**5.38%**
Mono->Substrate	Mono 40	Substrate 10	1.45%
Mono->Non-TWR	Mono 40	Non-TWR 20	0.67%
Mono->Mixed	**Mono 40**	**Mixed 30**	**11.04%**
No Change	Same	Same	73.86%

Table 14. Change detection from August 2020 to September 2020. Top three largest changes are in bold. Class mapping codes are included with the class name

Class Change	August Class	September Class	Percent
Substrate->Non-TWR	Substrate 10	Non-TWR 20	0.10%
Substrate->Mixed	Substrate 10	Mixed 30	3.55%
Substrate->Mono	**Substrate 10**	**Mono 40**	**5.11%**
Non-TWR->Substrate	Non-TWR 20	Substrate 10	0.15%
Non-TWR->Mixed	Non-TWR 20	Mixed 30	1.15%
Non-TWR->Mono	Non-TWR 20	Mono 40	0.21%
Mixed->Substrate	Mixed 30	Substrate 10	0.88%
Mixed->Non-TWR	Mixed 30	Non-TWR 20	0.72%
Mixed->Mono	**Mixed 30**	**Mono 40**	**11.75%**
Mono->Substrate	Mono 40	Substrate 10	0.84%
Mono->Non-TWR	Mono 40	Non-TWR 20	0.27%
Mono->Mixed	**Mono 40**	**Mixed 30**	**7.48%**
No Change	Same	Same	67.79%

Table 15. Change detection from July 2020 to September 2020. Top three largest changes are in bold. Class mapping codes are included with the class name.

Class Change	July Class	September Class	Percent
Substrate->Non-TWR	Substrate 10	Non-TWR 20	0.11%
Substrate->Mixed	Substrate 10	Mixed 30	3.55%
Substrate->Mono	**Substrate 10**	**Mono 40**	**6.66%**
Non-TWR->Substrate	Non-TWR 20	Substrate 10	0.11%
Non-TWR->Mixed	Non-TWR 20	Mixed 30	1.14%
Non-TWR->Mono	Non-TWR 20	Mono 40	0.23%
Mixed->Substrate	Mixed 30	Substrate 10	0.68%
Mixed->Non-TWR	Mixed 30	Non-TWR 20	0.33%
Mixed->Mono	**Mixed 30**	**Mono 40**	**8.05%**
Mono->Substrate	Mono 40	Substrate 10	0.78%
Mono->Non-TWR	Mono 40	Non-TWR 20	0.42%
Mono->Mixed	**Mono 40**	**Mixed 30**	**10.98%**
No Change	Same	Same	66.93%

V. DISCUSSION

Field Collection

Limitations in field collection were primarily due to weather and image acquisition. Initially, this study was going to be an analysis of anthropogenic impacts during the busiest season of the year, summer of 2020, but the circumstances due to COVID-19 prevented public river access and dramatically reduced the load of recreational users on the river. In the field, the team that collected the sUAS data dealt with issues from the weather due to heat and spectral responses. The time period during which flights occurred, July-September, are the hottest months in Texas and at times flights would be conducted in 100˚F+. Excessive heat prevented the sUAS from taking off, required a cool down and the use of multiple batteries, and is another reason why two flights were conducted during each data acquisition session. Despite attempting to fly at similar times of the day that experienced similar illumination conditions, when flying in a dynamic environment, cloud coverage changed the lighting of the landscape midflight, and this caused differences in spectral responses. The sUAS does have the ability to change the ISO and shutter speed midflight which can increase the brightness, but only when it was not taking photos. During a flight, the sUAS was programmed to take images every two seconds; at times because of the illumination conditions the ISO settings on the sUAS needed to be manually adjusted. There was a time delay between the transmitter and the sUAS, not all images had optimal exposure. Because of this, some imagery was darker and not optimal for use.

Lastly, despite public river access being closed, riverside businesses would allow river users to enter the river for a fee, and private river access never closed. As a result, for some of the images kayakers and swimmers obstructed the planar view of the river and increased water turbidity. The turbidity prevented the mapping of aquatic vegetation at specific sites, often a couple of meters in size and changed from month to month in both location and amount of river users present. In the July ortho, this totaled 9.7 M2 which totaled 0.11% of the total area, for the August ortho the total coverage amounted to 35.24 M2 which covered 0.40%of the image, and in September the coverage was 5.13 M2 amounting to 0.06% of the image's coverage. For future studies, I would recommend creating feature classes of polygon data that cover the recreational users to be used as a mask to avoid misclassifications.

Orthomosaics

While orthomosaics were chosen by their most optimal parameters for July and August, since there was only one image available to classify from September, I was expecting a lower Kappa and overall accuracy because the orthomosaic had cloud coverage and is darker overall than the July and August orthomosaics. The RMSE of the September imagery was much higher, which certainly affected the spatial accuracy of the data. In addition to the lowered brightness and higher RMSE, the September image features several "swirlies," or portions where the image becomes blurry due to distortion, which made classifying the image difficult. This type of distortion was previously reported by Chabot et al. (2017) and Pande-Chhetri et al. (2017) who specifically mentions the blurring of orthomosaic imagery and the resultant difficulty they encountered trying to classify emergent and submerged vegetation in low turbidity waters.

In general, capturing sUAS data in a dynamic environment proved to have challenges but can be accomplished if sufficient time is allocated to collect multiple sets of data. Flynn and Chapra (2014) identified difficulty capturing data in a windy environment and preventing off nadir or non-planar or directly above imagery by capturing images every two to five seconds. In this study, images were captured every two seconds and very few images were off-nadir. In the case of having off-nadir imagery in the data, those photos were removed prior to processing. In sum, capturing vegetation in a windy and spectrally changing environment created challenges, but the work can still be done with planning and repetition.

Reference Data

The data collected by BIO-WEST was a valuable resource for reference, but there were some differences in what was collected and what was visual in a planar view of the study area. After speaking with members of the Meadows Center for Water and the Environment (MCWE) habitat conservation crew, they confirmed the crew collects the data as viewed from a kayak in a similar planar fashion but from a much closer angle compared to the sUAS. Because of this difference in mapping, areas that were not documented to have TWR but visibly had it in the sUAS imagery or were confirmed to have TWR by the members of the MCWE habitat conservation crew were still considered Mono. An example is provided in Figure 6. The process of mapping each TWR stand present in the SMR can be nearly impossible due to the dynamic and at times rapid growth of the species. The BIO-WEST data in tandem with in-situ data collection and the continuous mapping of the SMR through remote sensing and GIS would likely create the most comprehensive overview of the coverage of TWR.

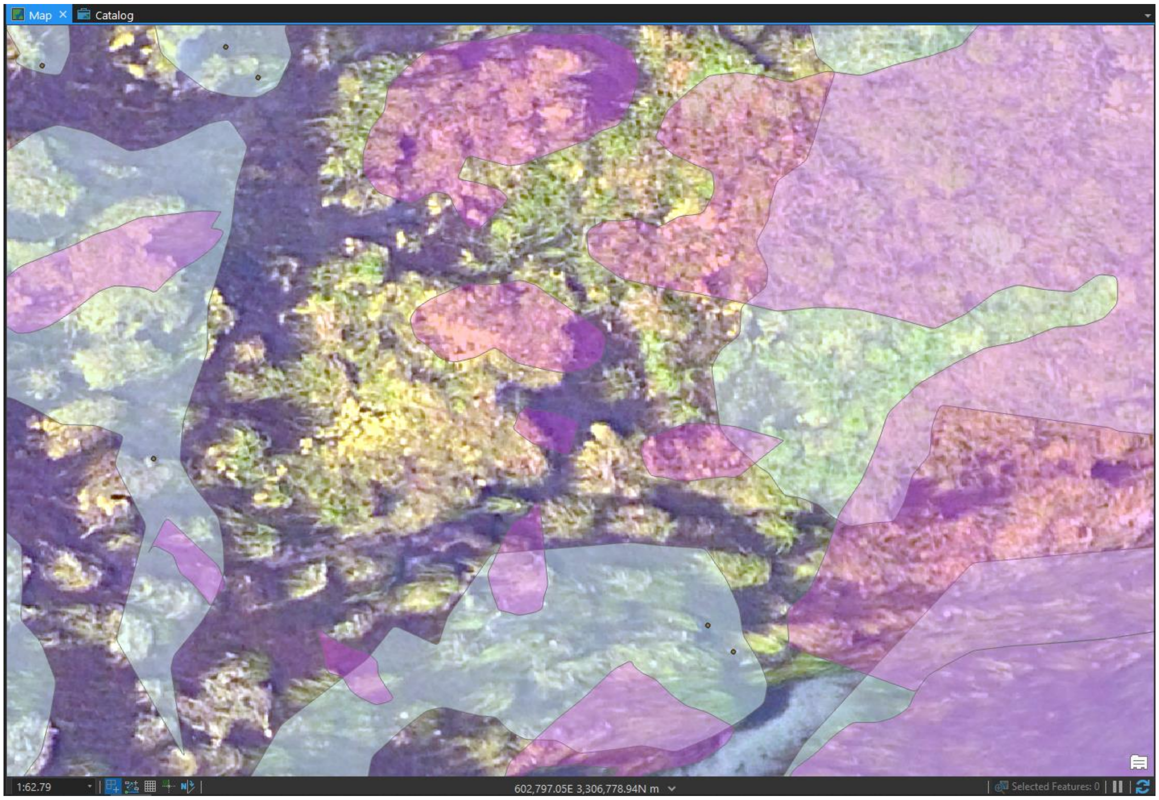

Figure 7 August 24,2020 orthomosaic with polygon data representing the mapped TWR from August 2019 (pink) and August 2020 (Blue). At the center are several bright green patches which have been confirmed to be Mono stands of TWR. This is not classified as TWR in the 2019 or 2020 data. The green patches were still classified as Mono based on interviews with the MCWE habitat conservation crew.

Image Classification

Within the study area there are three major locations where there are known mono stands: To the right directly below the Sewell Park bridge and above dog beach, to the left above City Park and adjacent to Dog Beach, and the remaining majority of the bottom image below Dog Beach. The central portion of the map, between Dog Beach and City Park is one of the major entrances and recreational swimming locations have experienced a large amount of contact recreation, which prevents the proliferation of aquatic species due to being trampled on. I believe the classified imagery visualize this accurately.

When classifying the imagery, the spectral responses of several macrophytes could be confused with TWR and other. Husson, Reese and Ecke (2017) also experienced issues when classifying taxa and they reported that spectrally similar aquatic vegetation will often be misclassified. To further understand the range of visible spectral responses in macrophytes, an aquatic plant table has been provided in Appendix 2.1. A suggestion for improvement on this work in the future would be to use a near infra-red (NIR) sensor to help interpret and classify vegetation rather than only using visible light in the electromagnetic spectrum. Chabot et al. (2018) and Jing et al. (2017) both reported improved classification accuracy after incorporating a NIR sensor in their works in low turbidity aquatic environments with submerged and semi-submerged macrophytes.

In addition to adding a NIR component, I would also suggest classifying smaller areas or sections of importance. One of the sections the EAHCP is focused on is below Sewell Park and above Dog Beach and is a diverse and dense location which could be studied on its own. Chabot et al. (2017) identified an issue of "under-segmentation" which is described as simplifying features through segmentation. A by-product of under-segmentation is data omission and was something that had to be balanced in this research. Finding the area between deriving objects of significance and avoiding noisy data might be easier to manage with a smaller study area. More time could be given to a smaller analysis extent for running a supervised classification and would potentially improve accuracy.

When in the field, it is clear that the classes are not clearly defined in the exact manner of the classified rasters, but rather there is a "transition" zone which is a mixture of vegetation slowly moving into the Mono. Non-TWR, or Mixed class. These transition zones are difficult to classify as there is no clear partition where one class begins and another one ends, and the similarity found with the visible view of vegetation in the river (Appendix 2.1). Because of this, and the common “mixed pixel” issue, where a pixel can contain two class types yet need to be assigned one class, there were certainly misclassifications in the data. Even with the ultra-high resolution of the data, some of these transition zones prevented difficulty in classifying the data, and this could be a source of error or uncertainty in both the classification and accuracy assessment steps of the research process. The use of an NIR component could help mitigate this as well as observations of the vegetation and their composition during the day of flights in future research.

Accuracy Assessments

Due to the issues with the September 2020 orthomosaic, I anticipated lower overall accuracy. Since TWR grows most rapidly during the spring and summer months (Powers and Poole 2004), finding classes that were entirely without TWR were not as frequent as the Mixed classes. Often the classes that were defined exclusively as Non-TWR represented less than three percent of the classified images coverage. This does not necessarily represent what is present on the ground, as there are areas where TWR has trouble rooting due to more clayey rock beds in the river (Saunders et al., 2001). However, this could be due to the growth of TWR in the time without large-scale anthropogenic impact, allowing the reach of the plant to cover the areas where TWR would not be present, making the planar view of the area to appear as a Mixed classification.

The overall accuracies and Kappa of the three images scored similar to the study done by Chabot et al. (2017) who reported overall accuracies ranging of 69.50% to 78.25% and Kappa values ranging from 0.47 to 0.60. However, these results are lower than Jing et al. (2017) who reported an overall accuracy of 88.89% and a Kappa of 0.86. These studies are used for comparison since they specifically used OBIA and RF to classify aquatic vegetation. The classified map accuracy was higher than the work done by Visser et al. (2016) who reported an overall accuracy range of 53% to 61%, however, their research attempted to specifically identify individual macrophytes rather than identifying vegetation composition like the work in this thesis does.

During in-situ surveys of the area, I saw locations where Water Pennywort (Hydrocoytle spp), a macrophyte that does not grow in the same location as TWR, had long leaves of TWR Mixed with it due to the large reach of a TWR plant growing several meters upstream from it and flowing down stream (Figure 7). This was evident in many areas of the orthomosaic creating a large Mixed class and may not be as visible in future studies due to resuming public access. In studies on how river users interact with TWR, it was often observed that the thin leaves of TWR are damaged most often by kayakers, swimmers and tubers ripping them out by their hands and paddles (Bradsby, 1996; Breslin, 1997), this will likely change the landscape of the study area.

Figure 8**.** Pennywort in the lower portion of the image, a macrophyte that roots in substrate that TWR does not prefer, mixed with TWR at the top portion of the image due to the reach of the TWR stand.

Because of the small percentage of Non-TWR class across all maps and the stratified random sampling design, all accuracy assessment points for the Non-TWR class amounted to 10 sample points per map. This created a varied range of accuracy assessment points, with 50% of Non-TWR points correctly classified in July (Table 10), and 100% correctly classified in September (Table 12). This did affect the Kappa values and overall accuracies for the maps. I would recommend creating a large sample size in the future for a more robust summary of the Non-TWR class.

Change Detection

Several caveats need to be made when interpreting the change detection maps and the percent class change. Specifically, what contraction and expansion truly represents, and what a planar view of the data provides compared to a three-dimensional view of aquatic vegetation. When looking at the change detection data and map, even if a class became smaller in size this does not necessarily mean that the class became smaller, but that growth of one class changed the planar view of the vegetation composition.

In all three change detections the same classes were identified as the largest percent changes: Substrate to Mono, Mixed to Mono and Mono to Mixed. While Substrate to Mono is a direct representation of root culm growth without being trampled on in the SMR (Poole, Powers, 2004) and the growth of matured TWR having an increased reach, Mono to Mixed and Mixed to Mono can seem contradictory. This Mixed to Mono change likely represents areas where a strong presence of TWR grew over and floated above the Mixed vegetation while areas with a heavier presence of Mixed vegetation grew as well in the Mono to Mixed change. The Mono to Mixed change could be an indicator of all species benefitting from the lack of river users during the summer of 2020, not just TWR. Additionally, the growth of the Mono class in any way can also be attributed to the growth of the species from matured stands gaining greater reach down stream, and the emergent root culms being large enough to be detected in the classification process.

The major change of pixels occurred around the dock directly below Sewell park, with the growth of the Mixed class identified in all three change detections. The growth of the Mono class occurred in excess around the large patch of Mono stands to the left above dog beach and below the Sewell park bridge, and below the patch of Mono stands adjacent to Dog Beach and to the right above City Park. Between Dog Beach and City Park, in the location where there is known contact recreation which tramples the vegetation there is significant growth in the Mono class, representing both new plant growth and existing growth maturing and extending further downstream. Directly above and to the left of dog beach there is a large portion of mixed vegetation and this area experienced significant growth in the mixed class, spreading out further from the central point of the patch. Overall, most growth was exhibited form the center of the river stream rather than along the riverbanks edge in the imagery, indicating the lack of river users allowing the vegetation that would normally be ripped out, pulled apart or trampled on to grow from root culms, root without interference, and mature without being torn apart. Figure 1 could be used a reference to see what the area would look like during a time of unrestricted recreational image since the imagery is satellite data from 2019 in order to compare how the growth changed during the summer of 2020.

Morgan and Hodgson (2021) found that some pixels that were identified as changed could be attributed to shadow differences from mapping the vegetation at a different period. Despite attempting to fly during uniform solar illumination conditions, the high resolution of the data and cloud coverage could cause a pixel to be identified as Mixed dark instead of Mono dark. In general, Liu (2016) found improved success in using change detections frequently from year to year and month to month, noting improved accuracy in classifying the data, and improved accuracy in detailing change.

The Mixed class indicated whether there was a presence of TWR but does not provide insight on what percentage of the vegetation is covered by TWR compared to other aquatic vegetation. Because of this, in the change detection there is no way to determine whether the change of Mixed classes amounted to the expansion or contraction of TWR within the Mixed class. Future research could be done to expand upon the mixed class, by providing percentage composition of the mixed class with TWR to other aquatic vegetation

No planting occurred by the MCWE habitat conservation crew during the summer of 2020, so new culms that were identified can be attributed to the growth of the species however, the EAHCP did work on floating vegetation mat (veg mat) removal. Veg mats are mixed species that have broken off from rooted macrophytes or small floating species that come together and float above vegetation in the river. Veg mats form in areas of dense vegetation with low velocity and are considered harmful to the vegetation as it prevents sunlight from penetrating the surface of the river and reaching submerged vegetation and prevents the flow of oxygen. During summer 2020 veg mat removal occurred nine times in the study area (Figure 8, Table 13) with the MCWE habitat conservation crew removing over 6,400 square meters of veg mats. Removal contributed to the change from Mixed (30) to Mono (40) classes specifically in the month of August as the removal of veg mats reveal stands of TWR from the sUAS planar view. Veg mats affect TWR significantly, since large stands of TWR can create low velocity, which is where veg mats are usually found, and this serves as an optimal location for invasive species as well (EAHCP, 2019). Removal occurred within a three-day period during the capturing of July and September imagery, so I do not believe it played as large of a role as it does in the August orthomosaic imagery.

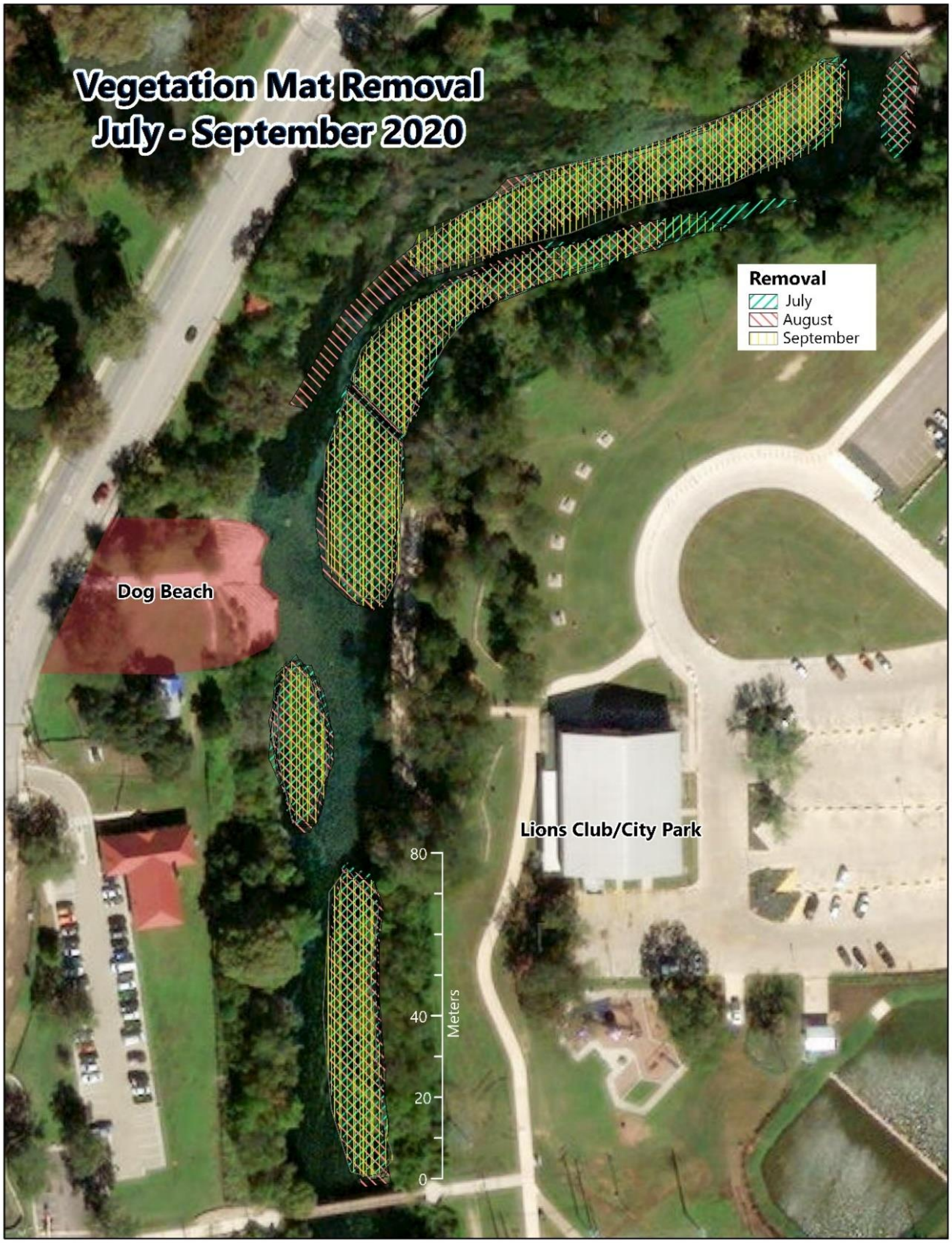

Figure 9. Vegetation mat removal that occurred during the study period by month. No veg mat removal occurred on data acquisition days.

Table 16. Dates of veg mat removal in study area and accumulated coverage of veg mat removal. The removed column represents the volume of veg mat removed in the area.

Comments	Date	Removed total (m^2)
Veg Mat Removed	07/04/20	321.15
Veg Mat Removed	07/11/20	811.55
Veg Mat Removed	07/18/20	769.63
Veg Mat Removed	07/23/20	721.23
Veg Mat Removed	08/12/20	1151.42
Veg Mat Removed	08/19/20	1032.84
Veg Mat Removed	08/27/20	601.01
Veg Mat Removed	09/15/20	673.66
Veg Mat Removed	09/22/20	407.51

VI. CONCLUSION

This research involved collecting sUAS imagery on an area of biological importance on the SMR during July, August, and September of 2020 to create continuous maps of vegetation in the SMR. One flight was processed from each month into an ultra-high resolution orthomosaic in Agisoft Metashape and an OBIA supervised classification was performed with the RF classifier to create classified imagery of the orthomosaics. Using reference data from GIS data, in-situ observations, in person interviews and over email, accuracy assessments were performed that yielded overall accuracies of 80.57% for July, 78.42% for August and 75.72% for September. The July and August classes had a Kappa above 0.61 indicating substantial agreement in accuracy and the September class had a Kappa of 0.59 indicating moderate agreement.

Change detections were performed on the classified maps from July to August, August to September, and July to September. All three change detections resulted in the same classes exhibiting the greatest change: Substrate to Mono indicating the growth of root culms and young TWR, Mixed to Mono indicating the growth of matured TWR and the removal of floating vegetation mats in the study area, and Mono to Mixed indicating the growth of all species during a time of little anthropogenic impact.

While this study involved developing a map of continuous coverage from a planar view, this study did not conduct a three-dimensional study of vegetation stands in the river, like the work BIO-WEST and the MCWE habitat conservation crew does on a regular basis. Mapping aquatic vegetation is impossible to do by planar view alone and will need to be corresponded with in-situ field work for validation and three-dimensional mapping to get a full contextual view of the composition of aquatic vegetation in a river system. This work could benefit from more in-situ observations at the time of data collection and additional reference data that could potentially be derived from sUAS with the help of an expert, or which could serve as a strong point of reference when assessing accuracy. The work done in this thesis along with the many other studies done on the SMR only represent parts of a dynamic, constantly changing river system.

An Analysis of Aquatic Vegetation in the San Marcos River Using sUAS contributes to a larger body of study on the endemic specie, TWR, on the SMR and can be used as a benchmark or reference as to the state of aquatic vegetation mapped in a continuous raster format for the summer months of 2020, which is normally when the river is experiencing the highest use. This work successfully implemented the use of OBIA in a low turbidity aquatic environment using sUAS to classify different aquatic vegetation compositions over the summer months during 2020 with change detections indicating the change of the vegetation from month to month and across the entire study period.

APPENDIX SECTION

APPENDIX 1.1: Orthomosaic July 13, 2020.

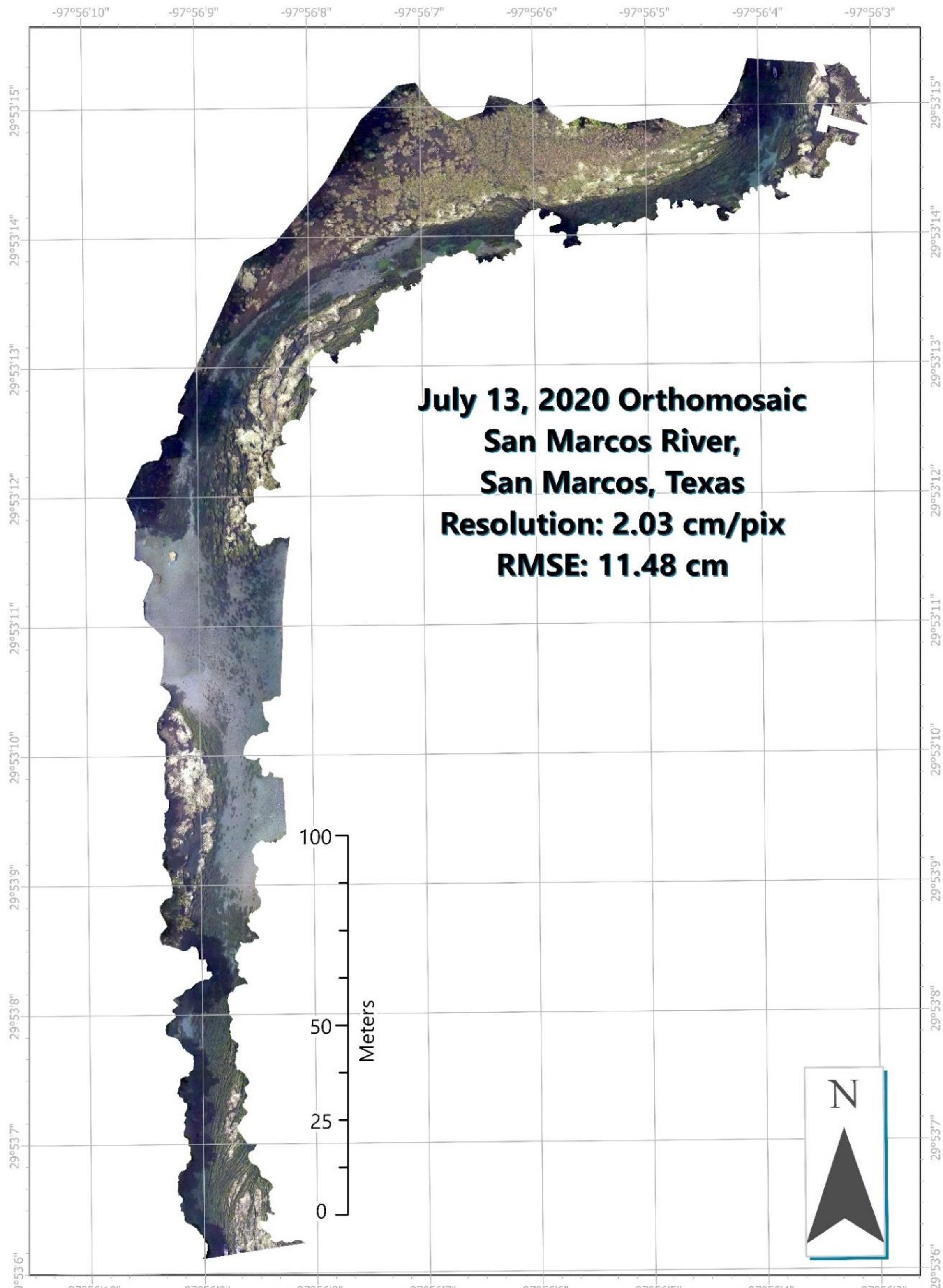

APPENDIX 1.2: Orthomosaic August 24, 2020.

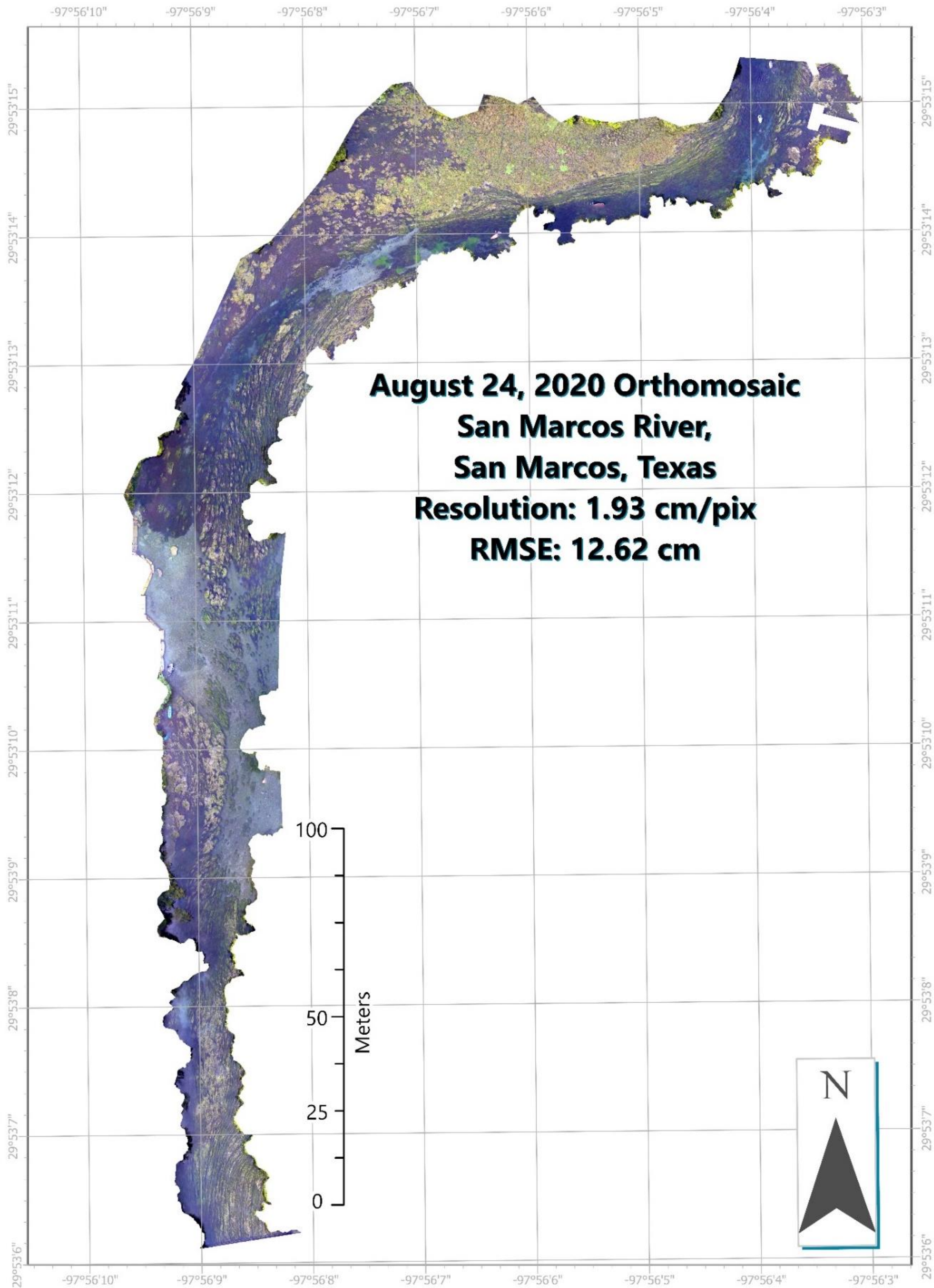

APPENDIX 1.3: Orthomosaic, September 25, 2020.

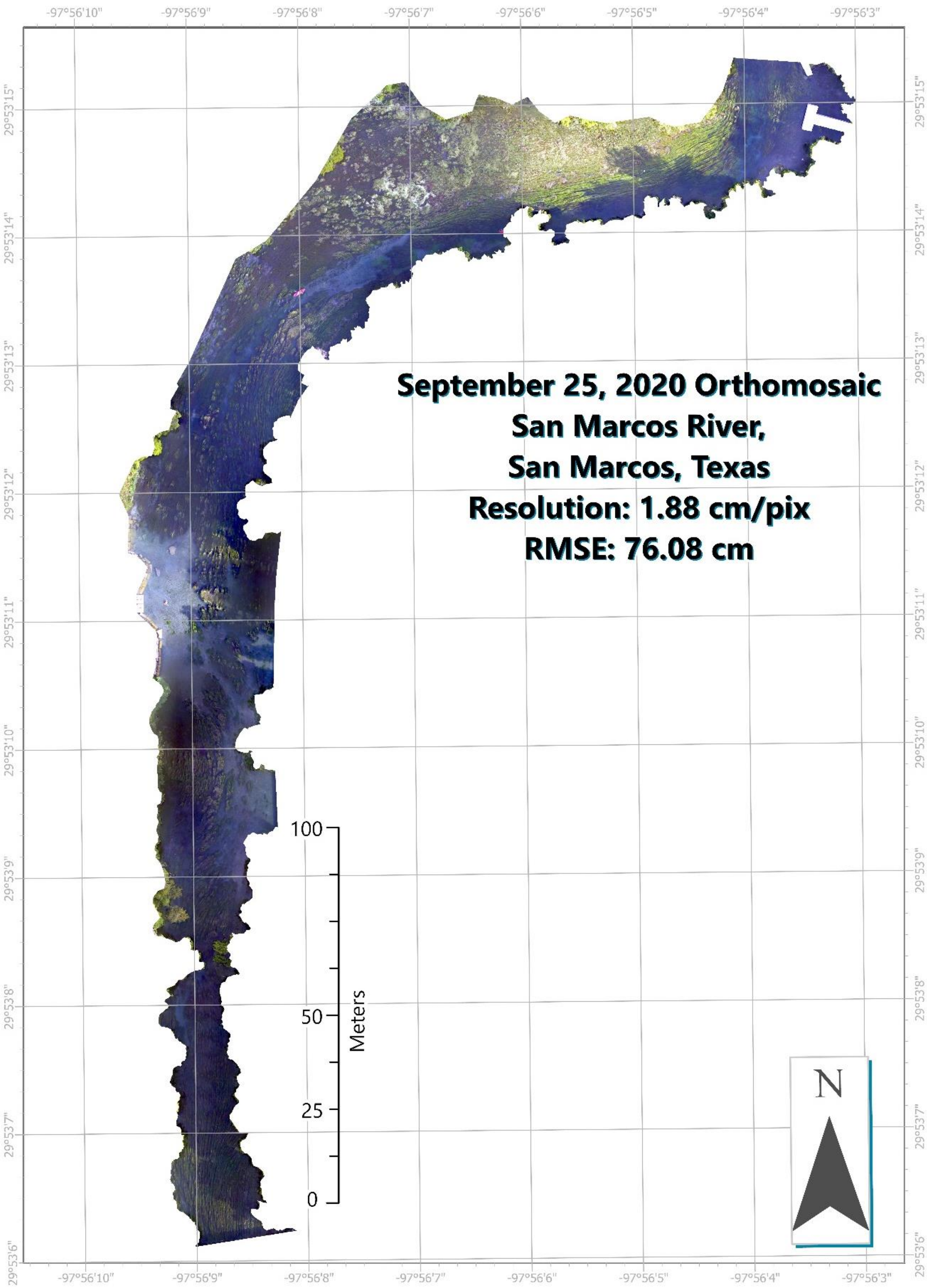

APPENDIX 2.1.0:

Name	Description	Size	Submerged/Floating?	Native/Invasive?	Image
Texas Wild rice ***(Zizania texana)***	Narrow grass macrophyte that can produce stalks above the water for reproduction. Can produce both sexually and asexually. This plant grows in stands and often roots in groups.	A strand can be 0.31 cm-2.5 cm wide and can become up to 40-200 cm long. Matured, adult plants average approximately 2.13 m long by 1 m wide.	**S**	**N**	Larger image can be found in Appendix 2.1.1
Coontail (Ceratophyllum demersum)	Identified by straight flat leaves, brittle stems that are branched and are somewhat cord-like and flexible. (AquaPlant, 2021). The coontail is a darker green but can sometimes appear brown in submerged water and is visibly able to be distinct from the spectral response of TWR.	The length of the coontail can range from 50 cm - 3.5 m, and as tall as the water column.	**Submerged, does not root into substrate, will float at surface.**	**N**	Larger image can be found in Appendix 2.1.2
Delta Arrowhead ***(Sagittaria platyphylla)*****:**	A broadleaf plant that is native to the eastern United States. The herb is perennial. Primarily submerged, the taller leaves can become emergent and rise above the water's surface.	The herb can range from 30 cm to 150 cm tall and the emerged leaves can range from 10 cm to 17 cm long.	**Begin submerged but leaves will emerge in shallow areas.**	**N**	Larger image can be found in Appendix 2.1.3
Illinois Pondweed ***(Potamogeton illinoensis***	A perennial plant. Pondweed has thin, elliptical shaped broad leaves, (AquaPlant, 2021). The stems are referred to as "runners" and found underground; it is red with a tinge of red at the base and branches out.	Leaves can be average 6-10 cm long and 2.5-3 cm wide, stems can grow to the entire water column.	**S**	**N**	Larger image can be found in Appendix 2.1.4
Water Pennywort ***(Hydrocoytle spp)***	Small perennial plant. Leaves are rounded, with stems attached to the center (TAPMS, 2020). Pennywort mainly grows in the locations of the riverbed that TWR is often not found, that include soft, clayey substrate. Referred to as a carpeting plant as it is found on the riverbed floor.	Averages 5 cm-7.62 cm submersed and 12.7 cm when out of the water and approximately 2 cm in diameter. Morphology changes based on flow of the river.	**Can grow fully out of the water and submerged.**	**N**	Larger image can be found in Appendix 2.1.5

APPENDIX 2.1.0 (Continued)

Name	Description	Size	Submerged/Floating?	Native/Invasive?	Image
Common Duckweed *(Lemna minor L.)*	Small, individual aquatic species that are flat with single roots that cluster together in groups of two to five or more. Duckweed is often found floating on the surface and in floating vegetation mats in dense colonies (AquaPlant, 2021). Duckweed will normally be found mixed in with other aquatic vegetation or in floating vegetation mats.	.16-.32 cm in size.	**F**	**I**	Larger image can be found in Appendix 2.1.6
Bladderwort (*Utriculariaa gibba*)	Small, webbed like aquatic species that are rootless and form in mats. Appear bright green in color and often form in clumps. Forms in whorls, appears spongy in texture, with long thin stems and thin branched leaves. This plant is carnivorous and has air sacks that trap insects for energy. Fluctuates seasonally. Found in stagnant back water.	12.7 cm-30 cm in size.	**S**	**N**	Larger image can be found in Appendix 2.1.7
Floating Crystalwort *(Riccia fluitans)*	An aquarium plant that grows in tangled clumps or mats. Stem and leaves are indistinguishable (AquaPlant, 2021)	An average of .2 cm in size, found in floating veg mats.	**F**	**N**	Larger image can be found in Appendix 2.1.8
Filamentous Algae	Single cell algae that string together to form mat like threads, chains, or filaments. Often clinging to rocks and can float to the surface. Thick filamentous hair algae, found in clay dominant substrate.	Size varies	**S & F**	**N**	Larger image can be found in Appendix 2.1.9

APPENDIX 2.1.0 (Continued)

Name	Description	Size	Submerged/Floating?	Native/Invasive?	Image
***Carolina Fanwort* (Cobomba caralliniana)**	Cylindrical stems with a thin, jelly like coating, that have leaf shape fans that come out in whorls. Appears similar to the coontail but it is slightly larger in size, the leaves are more feather like (AquaPlant, 2021).	Can grow to the length of the water column.	**S**	**N**	Larger image can be found in Appendix 2.1.10
Indian Hygrophila *(Hygrophila polysperma)*	A perennial plant that is native to India and Malaysia. The plant is found mostly submerged. (ERSS, 20XX). This plant can be confused with the native *Ludwigia repens* due to its red coloration from sun exposure. Hygrophila is aggressive. Can grow in riparian areas.	Leaves are normally .5-2.54 cm wide and 5-12.7 cm long.	**S**	**I**	Larger image can be found in Appendix 2.1.11
Water Thyme *(Hydrilla verticillata)*	This is a slender stemmed submerged plant from Africa that grows in whorls and is often found rooted in silty conditions trapping sediment. Hydrilla is also considered aggressively invasive. *Hydrilla* is often compared to looking closely like other watermilifoil species (TPWD, 2019). Differentiating between *Hydrilla* and *Elodea*, a lake plant can be nearly impossible without physical sampling.	Averages 5 cm in width and 6 m long.	**S**	**I**	Larger image can be found in Appendix 2.1.12

APPENDIX 2.1.0 (Continued)

Name	Description	Size	Submerged/Floating?	Native/Invasive?	Image
Floating Vegetation Mats	This is a mixture of species that have joined together to make large mats of floating vegetation. Dominated by Horntwort. A mixture of aquatic species can be found within the veg mats. Veg mats can prevent the flow of oxygen and can prevent sun rays from reaching the submerged vegetation, so they are routinely removed by the EAHCP. TWR and veg mats are commonly found near one another as TWR is the primarily emersed species on the river. Can submerge around TWR plants.	Size varies	**F**	**Predominantly composed of native species, some floating invasives might be found.**	Larger image can be found in Appendix 2.1.13
Water Lettuce *(Pistia stratiotes L.)*	Thick hearty leaves make up the floating emergent portion of this plant. Water Lettuce is clustered on very short branches with roots found in the water. The plant points upwards and fans out (AquaPlant, 2021)	Can be 25.4 cm in diameter. Can be 5-15 cm in height (Aquaplant, 2021).	**F**	**I**	Larger image can be found in Appendix 2.1.14
Watersprite *(Ceratopteris thalictroides)*	With leaves that resemble a fern, this is a fast growing invasive species that originated from the Philippines. The macrophyte normally has singular stems that have finger like leaves which can become numerous in a short amount of time (AquaPlant, 2021). When emerged the stalks can become.	The leaf structure of watersprite average 7.62 cm long and 2.5 cm wide. Can grow fully submerged rooted in substrate on the bed of the river.	**S & F**	**I**	Larger image can be found in Appendix 2.1.15

APPENDIX 2.1.0 (Continued)

Name	Description	Size	Submerged/Floating?	Native/Invasive?	Image
Watercress *(Nasturtium officinale)*	A perennial plant native to Europe and Asia, the plant has rounded leaves attached to a cylindrical stem. Roots occur at the nodes of the macrophyte and are stringy and thin in appearance (AquaPlant, 2021). Root structures can damage TWR through strangulation.	Leaves are an average of 2 cm in length and stems can reach a length anywhere from 9 cm to 58 cm long.	**F**	**I**	Larger image can be found in Appendix 2.1.16
Water Hyacinth (Eichhornia crassipes)	Originally from South America, water hyacinth is an aggressive invasive species that grows rapidly. This plant is identified by its blue to purple flowers, with round leathery leaved attached to inflated stalks (Aquaplant, 2021). Has long roots that hang below the plant mass.	The plant can grow an average of 12.5 cm tall and 10.2 cm wide.	**F**	**I**	Larger image can be found in Appendix 2.1.17
Water Stargrass (Heteranthera dubia)	Stargrass does not have runners, it is a bushy species from the root base and appears like pondweed and TWR, with long stems from the base and thin stems that resemble individual grass blades.	Can take up entire water column, does not become emersed. Leaves average 1 cm in width.	**S**	**N**	Larger image can be found in Appendix 2.1.18
Creeping Primrose (Ludwigia Repens)	Perennial plant that is elliptical shaped and red in color. This macrophyte has hardy cylindrical stems that are reddish brown in color. Roots are creeping and found at the nodes of the plant which gives the common name to the species. Riparian, capable of growing out of the water.	Stems can 30 cm to 53.34 cm long, and up to 2 to 5 cm wide.	**Submersed, but can grow fully out of the water.**	**N**	Larger image can be found in Appendix 2.1.19

APPENDIX 2.1.1: Texas Wild rice (*Zizania texana*)

Source: Alexa Lopez

APPENDIX 2.1.2: Coontail *(Ceratophyllum demersum)*

Source: Alexa Lopez

APPENDIX 2.1.3: Delta Arrowhead *(Sagittaria platyphylla)*

Source: Peggy Romfh. USDA, NRCS. 2018. The PLANTS Database (http://plants.usda.gov, 28 March 2018). National Plant Data Team, Greensboro, NC 27401-4901 USA.

APPENDIX 2.1.4: Illinois Pondweed *(Potamogeton illinoensis)*

Source: USDA, NRCS. 2021. The PLANTS Database (http://plants.sc.egov.usda.gov, 05/17/2021). National Plant Data Team, Greensboro, NC USA.

APPENDIX 2.1.5: Water Pennywort *(Hydrocoytle spp)*

Source: Alexa Lopez

APPENDIX 2.1.6: Common Duckweed *(Lemna minor L.)*

Among this pile of vegetation Duckweed can be seen, it is the bright green vegetation scattered throughout the image. Source: Alexa Lopez

APPENDIX 2.1.7: Bladderwort *(Utriculariaa gibba)*

Source: Rob Routledge, Sault College, Bugwood.org

APPENDIX 2.1.8: Floating Crystalwort *(Riccia fluitans)*

Source: University of Florida/IFAS Center for Aquatic and Invasive Plants.

APPENDIX 2.1.9: Filamentous Algae

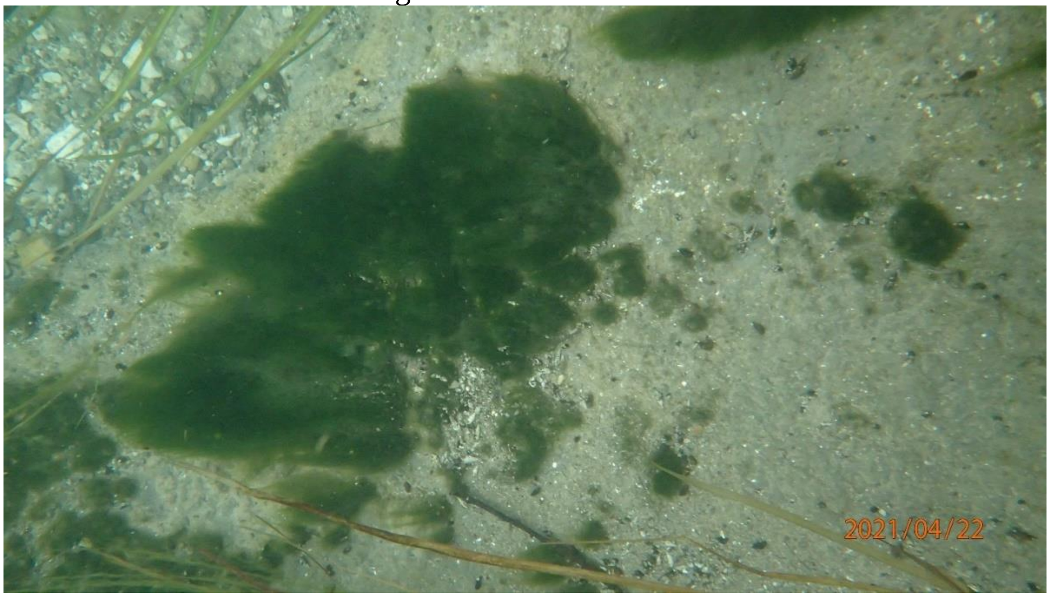

Source: Alexa Lopez

APPENDIX 2.1.10: Carolina Fanwort *(Cobomba caralliniana)*

Source: Alexa Lopez

APPENDIX 2.1.11: Indian Hygrophila *(Hygrophila polysperma)*

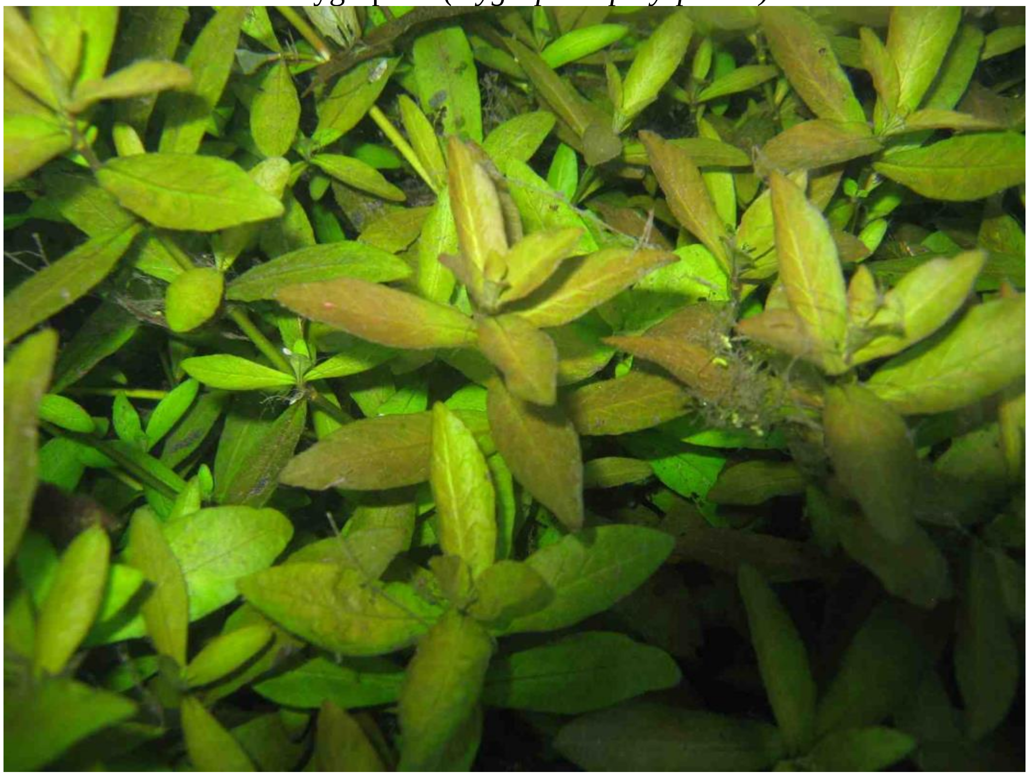

Source: USDA, NRCS. 2018. The PLANTS Database (http://plants.usda.gov, 28 March 2018). National Plant Data Team, Greensboro, NC 27401-4901 USA.

APPENDIX 2.1.12: Water Thyme *(Hydrilla verticillata)*

Source: Robert Videki, Doronicum Kft., Bugwood.org

APPENDIX 2.1.13: Floating Vegetation Mats

Source: Alexa Lopez

APPENDIX 2.1.14: Water Lettuce *(Pistia stratiotes L.)*

Source: Alexa Lopez

APPENDIX 2.1.15: Watersprite *(Ceratopteris thalictroides)*

Source: Alexa Lopez

APPENDIX 2.1.16: Watercress *(Nasturtium officinale)*

Source: Leslie J. Mehrhoff, University of Connecticut, Bugwood.org

APPENDIX 2.1.17: Water Hyacinth *(Eichhornia crassipes)*

Source: Peggy Romfh. USDA, NRCS. 2018. The PLANTS Database (http://plants.usda.gov, 28 March 2018). National Plant Data Team, Greensboro, NC 27401-4901 USA.

APPENDIX 2.1.18: Stargrass *(Heteranthera dubia)*

Source: Dean Wm. Taylor. Calscape. California Native Plant Society. 2014

APPENDIX 2.1.19: Creeping Primrose *(Ludwigia Repens)*

Source: Alexa Lopez

APPENDIX 3.0: Habitat conservation measures by the EAHCP.

Measures

— Texas wild ricewild rice Enhancement and Restoration (EAHCP §§ 5.3.1/5.4.1)

— Management of Recreation in Key Areas (EAHCP §§ 5.3.2/5.4.2)

— Management of Aquatic Vegetation and Litter Below Sewell Park (EAHCP § 5.3.3)

— Prohibition of Hazardous Materials Transport Across the San Marcos River and Its Tributaries (EAHCP § 5.3.4)

— Reduction of Non-Native Species Introduction (EAHCP §§ 5.3.5/5.4.11)

— Designation of Permanent Access Points/Bank Stabilization (EAHCP § 5.3.7)

— Control of Non-Native Plant Species (EAHCP §§ 5.3.8/5.4.3/5.4.12)

— Control of Harmful Non-Native and Predator Species (EAHCP §§ 5.3.9/5.4.13)

— Management of Floating Vegetation Mats and Litter (EAHCP §§ 5.3.3/5.4.3)

— Management of Golf Course and Grounds (EAHCP § 5.4.9)

— Native Riparian Restoration (EAHCP § 5.7.1)

— Impervious Cover/Water Quality Protection (EAHCP § 5.7.6)

— Management of Household Hazardous Wastes (EAHCP § 5.7.5)

— Prohibition of Hazardous Material Transport (EAHCP § 5.3.4)

REFERENCES

Alexander, Mara L. and Phillips, Catherine T. *Habitats Used by the Endangered Fountain Darter (Etheostoma Fonticola) in the San Marcos River, Hays County, Texas*. The Southwestern Naturalist 2012. 449-452.

Associates, Balanton &. *March 27, 2020. Edwards Aquifer Habitat Conservation Plan Annual Report.* U.S. Fish & Wildlife Service, 2020. Breslin, Shannon L.. December, 1997. Thesis: *The Impact Of Recreation on Texas Wild rice.* Texas State University. 1-131.

Bartsch, Nathan R., Hardy, Thomas B., Shoemaker, James P. *Development and Application of an Instream Flow Assessment Framework for the Fountain Darter (Etheostoma Fonticola) and Texas Wild rice (Zizania Texana) in Spring Lake and the San Marcos River System.* U.S. Fish and Wildlife Service. 1999. 2-38.

Bradsby, David D.. May, 1994. Thesis: *A Recreational Use Survey of the San Marcos River.* Texas State University. 1-71.

Breiman, Leo. *Random Forests*. Machine Learning 45, no. 1 (2001): 5-32.

Chabot, Dominique, Christopher Dillon, Oumer Ahmed, and Adam Shemrock. *Object-based analysis of UAS imagery to map emergent and submerged invasive aquatic vegetation: A case study.* Journal of Unmanned Vehicle Systems. 2017. 27-32.

Chabot, Dominique, Christopher Dillon, Adam Shemrock, Nicholas Weissflog, and Eric Sager. *An Object-Based Image Analysis workflow for monitoring shallow-water aquatic vegetation in multispectral drone imagery*. ISPRS International Journal of Geo-Information. 2018. 2-15.

City of New Braunfels. 2020. Website: *Comal River Rules & Tubing Information.* https://www.playinnewbraunfels.com/tube-in-new-braunfels/comal-river-rules/.

Dean Wm. Taylor. Calscape. Website: California Native Plant Society. 2014

Dynowski, Piotr, Adam Senetra, Anna Źróbek-Sokolnik, and Jacek Kozłowski. *The impact of recreational activities on aquatic vegetation in alpine lakes.* Water – Open Access Journal. 2019. 1-17.

ERSI, Inc.. 2021. Website: *Train Random Trees Classifier*. https://desktop.arcgis.com/en/arcmap/latest/tools/spatial-analyst-toolbox/train-random-trees-classifier.htm.

ESRI Inc.. 2021. Website: *Segmentation.* https://pro.arcgis.com/en/pro-app/latest/help/analysis/image-analyst/segmentation.htm.

Ewing, Thomas E. *Landscapes, Water and Man: Geology and History in the San Antonio area of Texas.* South Texas Geological Society. 2008.

Flynn, Kyle F., and Steven C. Chapra. *Remote Sensing of Submerged Aquatic Vegetation in a Shallow Non-turbid River Using an Unmanned Aerial Vehicle.* Journal: Remote Sensing. 2014. 12,817-12,831.

Grayson R. Morgan & Michael E. Hodgson (2021) A Post-Classification Change Detection Model with Confidences in High Resolution Multi-Date sUAS Imagery in Coastal South Carolina, International Journal of Remote Sensing, 42:11, 4309-4336.

Hardy, Thomas B. *Technical Assessments in Support of the Edwards Aquifer Science Committee "J charge" Flow Regime Evaluation for the Comal and San Marcos River Systems.* River Systems Institute: Texas State University. 2009. 1-159.

Hill, David J., Catherine Tarasoff, Garrett E. Whitworth, Jackson Baron, Jacob L. Bradshaw, and John S. Church. *Utility of Unmanned Aerial Vehicles for Mapping Invasive Plant Species: A Case Study on Yellow Flag Iris (iris pseudacorus L.).* International Journal of Remote Sensing: Unmanned Aerial Vehicles for Environmental Applications. 2017. 2,083-2,101.

Husson, Eva, Frauke Ecke, and Heather Reese. *Comparison of manual mapping and automated Object-Based Image Analysis of non-submerged aquatic vegetation from very-high-resolution UAS images*. Journal: Remote Sensing 2016. 1-18.

Husson, Eva, Heather Reese, and Frauke Ecke. *Combining spectral data and a DSM from UAS-images for improved classification of non-submerged aquatic vegetation*. Journal: Remote Sensing. 2017. 1-15.

Jensen, John R. 2005. Introductory Digital Image Processing: A Remote Sensing Perspective 3rd Ed; . Prentice Hall Series in Geographic Information Science. United States of America: Prentice Hall.

Jing, Ran, Zhaoning Gong, Wenji Zhao, Ruiliang Pu, and Lei Deng. *Above-bottom Biomass Retrieval of Aquatic Plants with Regression Models and SfM data acquired by a UAV platform – A Case Study in Wild Duck Lake Wetland, Beijing, China.* ISPRS Journal of Photogrammetry and Remote Sensing. 2017. 122-133.

Liu, Xiaohan, Yunlin Zhang, Kun Shi, Yongqiang Zhou, Xiangming Tang, Guangwei Zhu, and Boqiang Qin. *Mapping Aquatic Vegetation in a Large, Shallow Eutrophic lake: A frequency-based approach using multiple years of MODIS data*. Remote Sensing. 2015. 10,296-10,316.

Leslie J. Mehrhoff, University of Connecticut. *Watercress.* Website: Bugwood.org. 2014.

Ma, Lei, Manchun Li, Xiaoxue Ma, Liang Cheng, Peijun Du, and Yongxue Liu. *A Review of Supervised Object-based Land-cover Image Classification*. ISPRS Journal of Photogrammetry and Remote Sensing. 2017. 278-291.

Mora, Miguel A., William E. Grant, Leann Wilkins, and Hsiao-Hsuan Wang. Simulated Effects of Reduced Spring Flow from the Edwards Aquifer on Population Size of the Fountain Darter (etheostoma fonticola). Journal: Ecological Modelling. 2013. 250-243.

Musgrove, MaryLynn, and Cassi L. Crow. *Origin and Characteristics of Discharge at San Marcos Springs Based on Hydrologic and Geochemical Data (2008–10), Bexar, Comal, and Hays Counties, Texas.* U.S. Geologial Survey. 2011. 1-89.

Olsen, Jeffrey, Kinziger, Andrew, Wenburg, John, Lewis, Cara, Phillips, Catherine and Ostrand, Kenneth. *Genetic Diversity and Divergence in the Fountain Darter (Etheostoma Fonticola): Implications for Conservation of an Endangered Species. Journal:* Conservation Genetics. 2016. 1,393-1,404.

Owens, Chetta S., Madsen, John D., Smart, R. Michael, and Stewart, R. Michael. *Dispersal of Native and Nonnative Aquatic Plant Species in the San Marcos River, Texas*. Journal of Aquatic Plant Management. 2001. 75-79.

Peggy Romfh. USDA, NRCS. 2018. The PLANTS Database (http://plants.usda.gov, 28 March 2018). National Plant Data Team, Greensboro, NC 27401-4901 USA.

Pande-Chhetri, Roshan, Abd-Elrahman, Amr, Liu, Tao, Morton, Jon and Wilhelm, Victor L.. *Object-based Classification of Wetland Vegetation Using Very High-resolution Unmanned Air System Imagery*. European Journal of Remote Sensing. 2017. 564-576.

Qing, Song, A, Runa, Shun, Buri, Zhao, Wenjing, Bao, Yuhai, and Hao, Yanling. *Distinguishing and Mapping of Aquatic Vegetations and Yellow Algae Bloom with Landsat Satellite Data in a Complex Shallow Lake, China During 1986–2018*. Journal: Ecological Indicators. 2020. 1-16.

Reibe, et al, Board, Water Science and Technology, Studies, Division on Earth and Life, National Research Council, and Plan, Committee to Review the Edwards Aquifer Habitat Conservation. Review of the Edwards Aquifer Habitat Conservation Plan. Washington, D.C: National Academies Press. 2015. 1-186.

Robert Videki, Doronicum Kft. *Water Thyme.* Website: Bugwood.org. 2017

Rosińska, Joanna, and Gołdyn, Ryszard.. *Response of Vegetation to Growing Recreational Pressure in the Shallow Raczyńskie Lake.* Knowledge & Management of Aquatic Ecosystems. 2018. 1-8.

Rusnák, Miloš, Sládek, Ján, Kidová, Anna, and Lehotský, Milan. *Template for High-resolution River Landscape Mapping Using UAV Technology*. Measurement. 2018. 139-151.

Saunders, Kenneth S., Mayes, Kevin B., Jurgensen, Tim A., Trungale, Joseph F., Kleinsasser, Leroy J., Aziz, Karim, Fields, Jacqueline E., Moss, Randall E.. An Evaluation of Spring Flows to Support the Upper San Marcos River Spring Ecosystem, Hays County, Texas. River Studies Report No. 16.. Resource Protection Division Texas Parks and Wildlife Department. August 2001. 1-28.

TAMU Aquaplant. 2021. Website: https://aquaplant.tamu.edu/

TXP, Inc. The Impact of River Tourism in the San Marcos Area. Prepared for the Greater San Marcos Partnership. Fall, 2017. 1-20. https://greatersanmarcostx.com/sites/default/files/files/TXP%20San%20Marcos%20River%20Tourism%20Report%202017.pdf

Texas Water Development Board. Reconnaissance of the chemical qualities of the surface waters of the Guadalupe River Basin, Texas. Report 88. Austin, Texas. 1968.

University of Florida/IFAS Center for Aquatic and Invasive Plants. 2016.

U.S. Census Bureau. 2017. Estimates of the Components of Resident Population Change: April 1, 2010 to July 1, 2016 - PEPTCOMP. Generated using American FactFinder. (Available: https:// factfinder.census.gov/ 08/14/2017). https://demographics.texas.gov/Resources/publications/2017/2017_09_14_UrbanTexas.pdf

USDA, NRCS. 2019. The PLANTS Database. Website: http://plants.usda.gov. National Plant Data Team, Greensboro, NC 27401-4901 USA

U.S. Department of the Interior. Water resource data for Texas. Part 1. Surface water records. U.S. Geologic Survey, Federal Bldg., Austin, Texas. 1967-71.

U.S. Fish And Wildlife Service. Proposed Endangered status for some 1700 U.S. vascular plant taxa. Federal Register 41 (117, IV) June 16 1976. 24523-24572.

Poole, J.M. *Interim report on conservation of the upper San Marcos ecosystem: Texas wildrice (Zizania texana).* Albuquerque, NM: U.S. Fish and Wildlife Service, Region 2. 1992.

Poole, J.M. Texas wild ricewild rice *(Zizania texana):* a brief overview. Texas Parks and Wildlife Department: Austin, Texas. 1993.

Poole, J. M., botanist. Interview by author, 28 November, Austin. Personal communication. Texas Parks and Wildlife Department, Austin. 1995.

Poole, J.M. and D. Bowles. *Final Report. Project No. 49: Texas Wild rice (Zizania Texana*) *habitat characterization.* Austin, Texas: Texas Parks and Wildlife Department. 1996.

Poole, J and D. Bowles. Habitat Characterization of Texas Wild rice (*Zizania texana),* an endangered aquatic macrophyte from San Marcos, Tx, US. Aquatic Conservation: Marine and Freshwater Ecosystems. 1999. 291-302.

Power, P. and P.J. Fonteyn, Effects of oxygen concentration and substrate on seed germination and seedling growth of Texas Wildrice (*Zizania texana*). The Southwestern Naturalists. 1995.1-4.

Power, P. Effects of current velocity and substrate composition on growth of Texas Wild rice (*Zizania texana*). Aquatic Botany. 1996. 55: 199-204

Power, P. Direct and Indirect effects of floating vegetation mats on Texas Wild rice (*Zizania texana*). The Southwestern Naturalists. 1998. 41 (4): 462-464.

Power, P.J. Moisture, Seeds, and Reproductive Failure in Texas Wild rice (*Zizania texana*). Southwestern Naturalists. 1997. 42 (4):435-440

Rob Routledge, Sault College. *Bladderwort* Website: Bugwood.org. 2014.

Silveus, W. A. Texas Grasses. The Clegg Company, San Antonio, Texas. 1933. 765-782.

Terrell, E.E., W. Emery, and H. Beaty. Observations on Zizania texana (Texas wild ricewild rice), and Endangered Species. Torrey Botanical Society. 1978. 105 (1): 50-57.

Tolman, Kristina.May, Thesis: *Habitat Characterization Of Zizania Texana In The San Marcos River.* Texas State University. 2013. 1-48.

USDA, NRCS. 2018. The PLANTS Database (http://plants.usda.gov, 28 March 2018). National Plant Data Team, Greensboro, NC 27401-4901 USA.

Young, W.C., B.G. Whiteside, G. Longley, and N.E. Carter.. The Guadalupe-San Antonio Nueces River Project. Phase1: Review of existing biological data. Final report to the Texas Water Development Board. 1973